# Arctic Tropospheric Ozone Trends

Kathy S Law[1], Jens Liengaard Hjorth[2], Jakob Boyd Pernov[3], Cynthia Whaley[4], Henrik Skov[2], Martine Collaud Coen[5], Joakim Langner[6], Steve Robert Arnold[7], David W Tarasick[8], Jesper Christensen[2], Makoto Deushi[9], Peter Effertz[10], Greg Faluvegi[11], Michael Gauss[12], Ulas Im[13], Naga Oshima[9], Irina Petropavlovskikh[14], David Plummer[15], Kostas Tsigaridis[16], Svetlana Tsyro[12], Sverre Solberg[17], and Steven T Turnock[18]

[1]Sorbonne Université (LATMOS)
[2]Interdisciplinary Centre for Climate Change, Aarhus University
[3]EPFL
[4]Environment and Climate Change Canada
[5]MeteoSwiss
[6]SMHI, Folkborgsvägen , 601 76 Norrköping, Sweden
[7]University of Leeds
[8]Environment and Climate Change Canada / Government of Canada
[9]Meteorological Research Institute
[10]CIRES, University of Colorado/NOAA Global Monitoring Laboratory
[11]Columbia University
[12]Norwegian Meteorological Institute
[13]Aarhus University
[14]Cooperative Institude for Research in Environmental Sciences, CU
[15]Environment Canada
[16]Center for Climate Systems Research, Columbia University, and NASA Goddard Institute for Space Studies
[17]Norwegian Institute for Air Research
[18]Met Office Hadley Centre

March 9, 2023

**Abstract**

Trends in tropospheric ozone, an important air pollutant and short-lived climate forcer (SLCF), are estimated using available surface and ozonesonde profile data for 1993-2019. Using a coherent methodology, observed trends are compared to modeled trends (1995-2015) from the Arctic Monitoring Assessment Programme SLCF 2021 assessment. Statistically significant increases in observed surface ozone at Arctic coastal sites, notably during winter, and concurrent decreasing trends in surface carbon monoxide, are generally captured by multi-model median (MMM) trends. Wintertime increases are also estimated in the free troposphere at most Arctic sites, but tend to be overestimated by the MMMs. Springtime surface ozone increases in northern coastal Alaska are not simulated while negative springtime trends in northern Scandinavia are not always reproduced. Possible reasons for observed changes and model behavior are discussed, including decreasing precursor emissions, changing ozone sinks, and variability in large-scale meteorology.

# Arctic Tropospheric Ozone Trends

K. S. Law[1], J. Liengaard Hjorth[2], J. B. Pernov[2,3], C. H. Whaley[4], H. Skov[2], M. Collaud Coen[5], J. Langner[6], S. R. Arnold[7], D. Tarasick[8], J. Christensen[2], M. Deushi[9], P. Effertz[10,14], G. Faluvegi[11,12], M. Gauss[13], U. Im[2], N. Oshima[9], I. Petropavlovskikh[10,14], D. Plummer[4], K. Tsigaridis[11,12], S. Tsyro[13], S. Solberg[15] and S.T. Turnock[16,7]

[1]Sorbonne Université, LATMOS-IPSL, UVSQ, CNRS, Paris, France
[2]Department of Environmental Science, Interdisciplinary Centre for Climate Change, Aarhus University, Frederiksborgvej 4000, Roskilde, Denmark
[3]Extreme Environments Research Laboratory, École Polytechnique Fédérale de Lausanne, 1951 Sion, Switzerland
[4]Canadian Centre for Climate modeling and analysis, Environment and Climate Change Canada, Victoria, BC, Canada
[5]Federal Office of Meteorology and Climatology, MeteoSwiss, Payerne, Switzerland
[6]Swedish Meteorological and Hydrological Institute, Norrköping, Sweden
[7]Institute for Climate and Atmospheric Science, School of Earth and Environment, University of Leeds, Leeds, United Kingdom
[8]Air Quality Research Division, Environment and Climate Change Canada, Toronto, ON, Canada
[9]Meteorological Research Institute, Japan Meteorological Agency, Tsukuba, Japan
[10]Cooperative Institute for Research in Environmental Sciences (CIRES), University of Colorado, Boulder, CO, USA.
[11]NASA Goddard Institute for Space Studies, New York, NY, USA
[12]Center for Climate Systems Research, Columbia University; New York, USA
[13]Norwegian Meteorological Institute, Oslo, Norway
[14]National Oceanic and Atmospheric Administration (NOAA) ESRL Global Monitoring Laboratory, Boulder, CO, USA.
[15]Norwegian Institute for Air Research (NILU), Kjeller, Norway.
[16]Met Office Hadley Centre, Exeter, UK

Corresponding author: Kathy.Law@latmos.ipsl.fr

## Key Points:

- Coherent ozone trend analysis methodology applied to multi-decade, pan-Arctic surface and ozonesonde datasets and multi-model medians.
- Increasing winter Arctic tropospheric ozone overestimated by models in the free troposphere, Alaskan spring surface increases not captured.
- Spring (summer) decreases (increases) in observed ozone throughout the troposphere, not always simulated by models.

# Abstract

Trends in tropospheric ozone, an important air pollutant and short-lived climate forcer (SLCF), are estimated using available surface and ozonesonde profile data for 1993-2019. Using a coherent methodology, observed trends are compared to modeled trends (1995-2015) from the Arctic Monitoring Assessment Programme SLCF 2021 assessment. Statistically significant increases in observed surface ozone at Arctic coastal sites, notably during winter, and concurrent decreasing trends in surface carbon monoxide, are generally captured by multi-model median (MMM) trends. Wintertime increases are also estimated in the free troposphere at most Arctic sites, but tend to be overestimated by the MMMs. Springtime surface ozone increases in northern coastal Alaska are not simulated while negative springtime trends in northern Scandinavia are not always reproduced. Possible reasons for observed changes and model behavior are discussed, including decreasing precursor emissions, changing ozone sinks, and variability in large-scale meteorology.

**Plain Language Summary**

The Arctic is warming much faster than the rest of the globe due to increases in carbon dioxide, and other trace constituents like ozone, also an air pollutant. However, improved understanding is needed about long-term changes or trends in Arctic tropospheric ozone. A coherent methodology is applied to determine trends in surface and regular profile measurements over the last 20-30 years, and results from six chemistry-climate models. Statistically significant increases in observed ozone are found at the surface and in the free troposphere during winter in the high Arctic. Paradoxically, decreases in nitrogen oxide emissions at mid-latitudes appear to be leading to increases in ozone during winter, but associated increases in Arctic tropospheric ozone tend to be overestimated in the models. Increases are also found at the surface in northern Alaska during spring but not reproduced by the models. The causes are unknown but could be related to changes in local sources or sinks of Arctic ozone or in large-scale weather patterns. Declining mid-latitude emissions may also explain negative surface ozone trends over northern Scandinavia in spring that are not always captured by the models. Further work is needed to understand changes in Arctic tropospheric ozone.


# 1 Introduction

Tropospheric ozone ($O_3$) is a short-lived climate forcer (SLCF) contributing to global and Arctic warming (AMAP, 2015; Sand et al, 2016; von Salzen et al. 2022), and a critical secondary air pollutant, detrimental to human health (Anenberg et al., 2010) and ecosystems (Arnold et al., 2018). The Arctic tropospheric $O_3$ budget is complex, as recently discussed in a companion paper, Whaley et al. (2023). It originates from photochemical production of anthropogenic or

natural emissions of $O_3$ precursors, including nitrogen oxides ($NO_x$), carbon monoxide (CO) and methane ($CH_4$), in the Arctic, or following air mass transport from mid-latitudes, as well as transport of $O_3$ from the stratosphere (Law et al., 2014; Schmale et al., 2018). Sinks include photochemical destruction, including reactions involving halogens leading to so-called ozone depletion events (ODEs) (Barrie, et al., 1988; Simpson et al., 2007), and surface dry deposition (Clifton et al., 2020). Growth in anthropogenic emissions since pre-industrial times has led to increases in tropospheric $O_3$ throughout the Northern Hemisphere (NH) (Tarasick et al., 2019; Turnock et al., 2020; Cooper et al., 2020) contributing to observed global and Arctic warming over the past century (e.g. Griffiths et al., 2021). Since the mid-1990s, a mix of relatively weak positive and negative trends (+1 to -1 parts per billion by volume (ppbv) per decade) have been reported in the NH at the surface and in the free troposphere (FT), with largest increases over south and eastern Asia, associated with increasing anthropogenic emissions (Cooper et al., 2020; Wang et al., 2022a).

To date, only a few studies have focused on assessing tropospheric $O_3$ trends in the Arctic. While positive $O_3$ trends were diagnosed at several surface sites, results are not always statistically significant, and both positive and negative trends were reported at some Canadian sites (Tarasick et al., 2016; Sharma et al., 2019; Cooper et al., 2020). In the Arctic FT, studies found significant positive trends (Christiansen et al., 2017; Wang et al., 2022a), no trends (Tarasick et al., 2016), or mixed trends in different seasons (Bahramvash Shams et al., 2019). Differences in the periods analyzed, sign or magnitude of trends emphasizes the need to further examine trends using the same methodology. Coherent estimation of observed trends, and evaluation of modeled trends, is needed to better understand $O_3$ changes and impacts on Arctic climate that are sensitive to the altitude where $O_3$ perturbations occur (Rap et al., 2015). This study assesses annual and monthly trends, together with possible evolution in seasonal cycles, of Arctic tropospheric $O_3$ over the last 20-30 years. Observed changes are compared to results from atmospheric chemistry-climate models run as part of the recent Arctic Monitoring and Assessment Programme (AMAP) SLCF assessment (AMAP, 2021; Whaley et al., 2022; von Salzen et al., 2022). Results are discussed in light of possible changes in sources and sinks of Arctic tropospheric $O_3$.

# 2 Methods

## 2.1 Measurements

The location of surface and ozonesonde sites used in this study are displayed in Fig. 1, together with the Arctic Circle at 66.6°N, used to define the Arctic. Annual surface trends are shown in the table grouped into 1) high Arctic coastal sites (Alert, Utqiaġvik/Barrow, Villum), Zeppelin (situated at 474m on Svalbard) and Summit (high altitude (FT) site on Greenland (3211m), and 2) European continental sites within (Pallas, Esrange), and just south (Tustervatn) of the Arctic Circle.


| Site | Annual trend (%) | Significance level | Period |
|---|---|---|---|
| ***High Arctic:*** | | | |
| Alert | **0.29** | 95% | 1999-2019 |
| | **0.24** | 95% | 1993-2019 |
| Utqiagvik | 0.53 | <90% | 1999-2019 |
| | 0.26 | <90% | 1993-2019 |
| Villum | **1.98** | 95% | 1999-2019 |
| | 0.68 | 90% | 1996-2019 |
| Zeppelin | -0.19 | <90% | 1999-2019 |
| | **0.18** | 90% | 1993-2019 |
| Summit | -0.28 | <90% | 2001-2019 |
| ***European continental Arctic and near-Arctic:*** | | | |
| Esrange | 0.08 | <90% | 1999-2019 |
| | 0.00 | <90% | 1993-2019 |
| Pallas | **-0.30** | 90% | 1998-2019 |
| | **-0.40** | 90% | 1995-2019 |
| Tustervatn | **-0.52** | 99% | 1999-2019 |
| | -0.18 | >90% | 1994-2019 |

***Figure 1.*** *Left: Location of surface (bold) and ozonesonde (italic) sites and showing the Arctic Circle (66.55°N). Right: annual $O_3$ trends at surface sites in % per year (left column), the significance level (middle column), calculated over periods shown in the right column. Statistically significant trends (above 90% confidence level) are in bold. Geographical coordinates for all sites are provided in Whaley et al. (2023). See text for details.*

Surface observations are from EBAS Level 2 data, station owners for Villum before 2001, Canada's Open Government Portal for Alert, and National Oceanic and Atmospheric

Administration (NOAA) for Summit, and Barrow Atmospheric Observatory, Utqiaġvik (Utqiaġvik from now on). Ozonesonde data are from the World Ozone and Ultraviolet Radiation Data Centre (WOUDC) and Network for the Detection of Atmospheric Composition Change (NDACC). See also the Supplementary Information (Text S1, Figs. S1 and S2, including data coverage).

### 2.2 Trend analysis

Observed monthly and annual trends in surface $O_3$ concentrations at different sites are determined using the non-parametric Mann-Kendall test at the $90^{th}$ and $95^{th}$ confidence level (CL) and Sen's slope methodology (Theil, 1950; Sen, 1968) (see Text S2). Daily median data are sorted into different months and pre-whitened, due to the presence of autocorrelation, via the 3PW algorithm from Collaud Coen et al. (2020). Trends using ozonesonde profiles are calculated based on weekly medians for selected pressure levels. For the calculation of relative trends, data are normalized by division with median values and multiplied by 100.

### 2.3 Modeled trends

Modeled trends at the surface and different altitudes are calculated for 1995-2015 using results from four global chemistry-climate models (CMAM, GISS-E2.1, MRI-ESM2, UKESM1) and two chemistry-transport models (DEHM, EMEP MSC-W) run using the same ECLIPSEv6b anthropogenic emissions, and nudged with meteorological reanalyses as part of AMAP (2021). Details can be found in Whaley et al. (2022), Text S3 and Table S1. Simulated monthly mean $O_3$ volume mixing ratios from the model grid box containing the measurement location are used to compute multi-model medians (MMMs). For ozonesonde comparisons, modeled vertical profiles are interpolated onto the same vertical bins as the measurements before trends are computed.

## 3 Surface ozone trends in the Arctic

### 3.1 Observed ozone trends

Annual trends are calculated for 1993-2019, or for the longest period with sufficient data, for all the sites (see Fig. 1, Table S2).

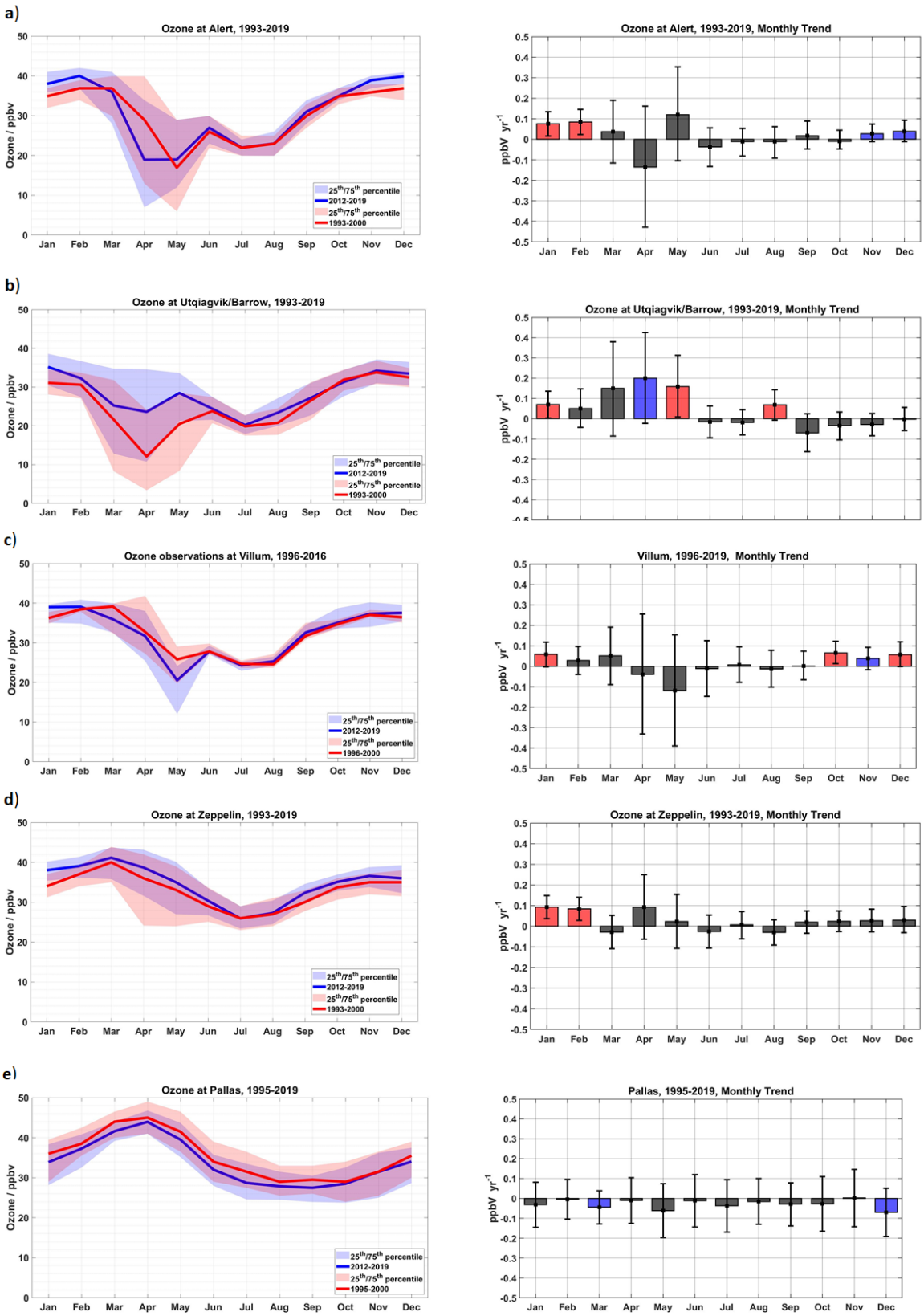
a)
Ozone at Alert, 1993-2019
Ozone / ppbv
25th/75th percentile
2012-2019
25th/75th percentile
1993-2000
Ozone at Alert, 1993-2019, Monthly Trend
ppbV yr-1
b)
Ozone at Utqiagvik/Barrow, 1993-2019
Ozone / ppbv
25th/75th percentile
2012-2019
25th/75th percentile
1993-2000
Ozone at Utqiagvik/Barrow, 1993-2019, Monthly Trend
ppbV yr-1
c)
Ozone observations at Villum, 1996-2016
Ozone / ppbv
25th/75th percentile
2012-2019
25th/75th percentile
1996-2000
Villum, 1996-2019, Monthly Trend
ppbV yr-1
d)
Ozone at Zeppelin, 1993-2019
Ozone / ppbv
25th/75th percentile
2012-2019
25th/75th percentile
1993-2000
Ozone at Zeppelin, 1993-2019, Monthly Trend
ppbV yr-1
e)
Ozone at Pallas, 1995-2019
Ozone / ppbv
25th/75th percentile
2012-2019
25th/75th percentile
1995-2000
Pallas, 1995-2019, Monthly Trend
ppbV yr-1
Jan Feb Mar Apr May Jun Jul Aug Sep Oct Nov Dec

***Figure 2.*** *Observed surface $O_3$ trends and seasonal cycles. Left: seasonal cycles of monthly median $O_3$ (ppbv) at a) Alert, b) Utqiaġvik, c) Villum, d) Zeppelin, and e) Pallas for 1993-2000 (blue lines) vs 2012-2019 (red lines). Shaded areas show upper and lower quartiles of hourly values. Right: monthly trends for 1993-2019. Boxes represent the slope of the trend in ppbv per year with red boxes significant at 95$^{th}$% CL, blue boxes at 90$^{th}$% CL, and black boxes not statistically significant. Error bars show 95$^{th}$% CLs. Results are shown for shorter periods depending on data availability.*

Average $O_3$ seasonal cycles are also calculated for earlier (1993-2000) and later (2012-2019) periods, to examine possible changes, together with monthly trends (Fig. 2) at selected sites (see Fig. S3 for other sites). Monthly trends are also analyzed for different 21-year periods (1993-2012, 1999-2019) (Fig. S4).

First considering high Arctic sites at coastal locations that exhibit a winter maximum with low spring concentrations attributed to ODEs, as discussed in Whaley et al. (2023). Alert has statistically significant ("ss") positive $O_3$ annual trends, as does Villum for the shorter time period 1999-2019, while annual trends at Utqiaġvik are not significant (see Fig. 1). Ss trends are also calculated in particular seasons, as shown in Fig. 2. Notably, ss positive trends are found during late autumn and/or winter at Alert, Villum and Utqiaġvik. Positive trends are also calculated for spring at Utqiaġvik (April-May). Winter trends at Alert and spring trends at Utqiaġvik are more pronounced when using the later record (1999-2019) (see Fig. S4). To further characterize these changes, probability distributions in observed $O_3$ concentrations are calculated for months with ss trends (see Fig. S5). Positive ss trends during winter and spring at Utqiaġvik are the result of a decrease (increase) in the frequency of low (high) concentrations (Jan.-May), whereas wintertime $O_3$ concentrations shifted recently towards higher values at Alert (Nov.-Feb.) and Villum (Oct.-Jan.). Zeppelin shows a different seasonal behavior compared to Arctic sea-level coastal sites with a spring maximum, more similar to remote mid-latitude sites. Here, ss positive annual trends are estimated for 1993-2019 (Fig. 1), and in winter (Fig. 2), driven by increases in the earlier part of the record (1993-2013) (Fig. S4).

Continental northern Scandinavian sites exhibit a different behavior with Pallas and Tustervatn showing ss negative annual trends but no ss annual (or monthly) trends at Esrange over any of the periods considered. The shape of the seasonal cycle for the earlier versus the later period is

similar at these sites, which also have a spring maximum like Zeppelin. $O_3$ appears to be decreasing throughout the year when comparing earlier and later periods although ss negative trends are only evident at Pallas (March, December), and at Tustervatn in spring and early summer (Fig. S4, 1999-2019 trends). Summit is more representative of the FT and samples air masses transported from North America and Asia, or of stratospheric origin (Dibb, 2007; Schmeisser et al., 2018). The annual trend, calculated over the shorter 2001-2019 record, is not ss at the 90$^{th}$ % CL, but ss negative monthly trends are estimated for January, March-May and September.

## 3.2 Comparison of observed and modeled surface trends

Figure 3 compares observed monthly and MMM trends for 1995-2015, or the closest possible time interval in case of years with missing observations. Results for other sites are shown in Fig. S6. Observed ss trends are more frequently diagnosed over 1993-2019 (Fig. 2) than over the shorter period ending in 2015 (Fig. 3). While the MMMs simulate $O_3$ seasonal cycles reasonably well, low $O_3$ concentrations are missed in spring, and wintertime $O_3$ is underestimated (Whaley et al., 2023). The MMMs simulate ss positive and negative trends at Zeppelin (Jan.) and Esrange (May), respectively, but not ss positive trends at Utqiaġvik (April). Ss trends are simulated, but not observed, at Alert (January, December) and Tustervatn (March).

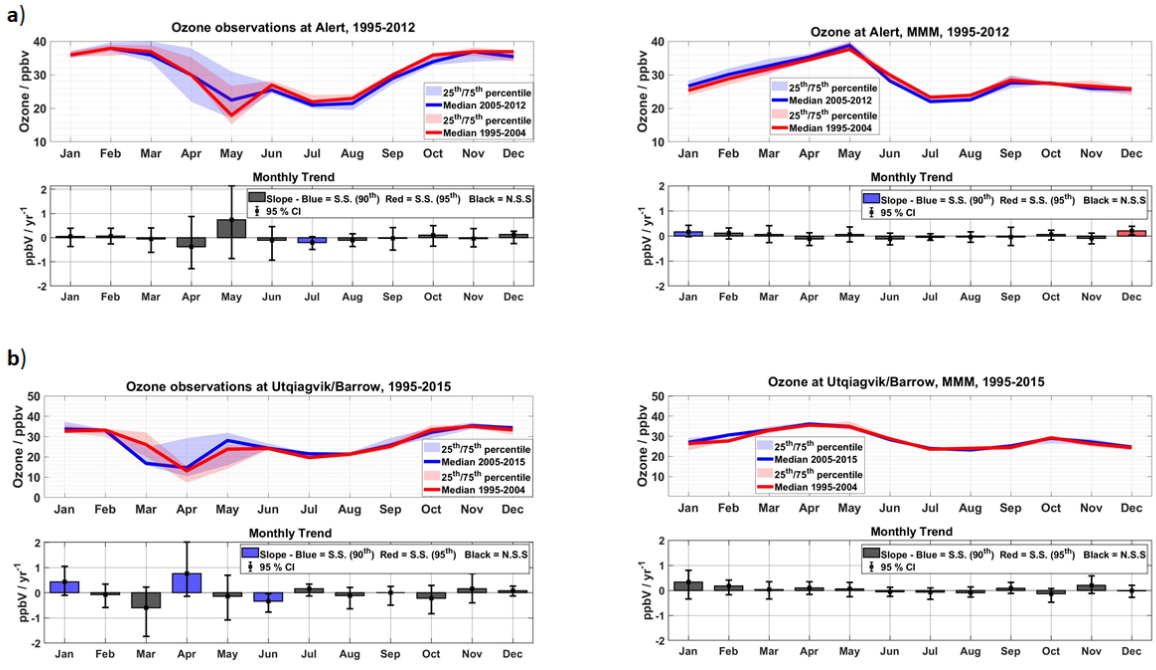

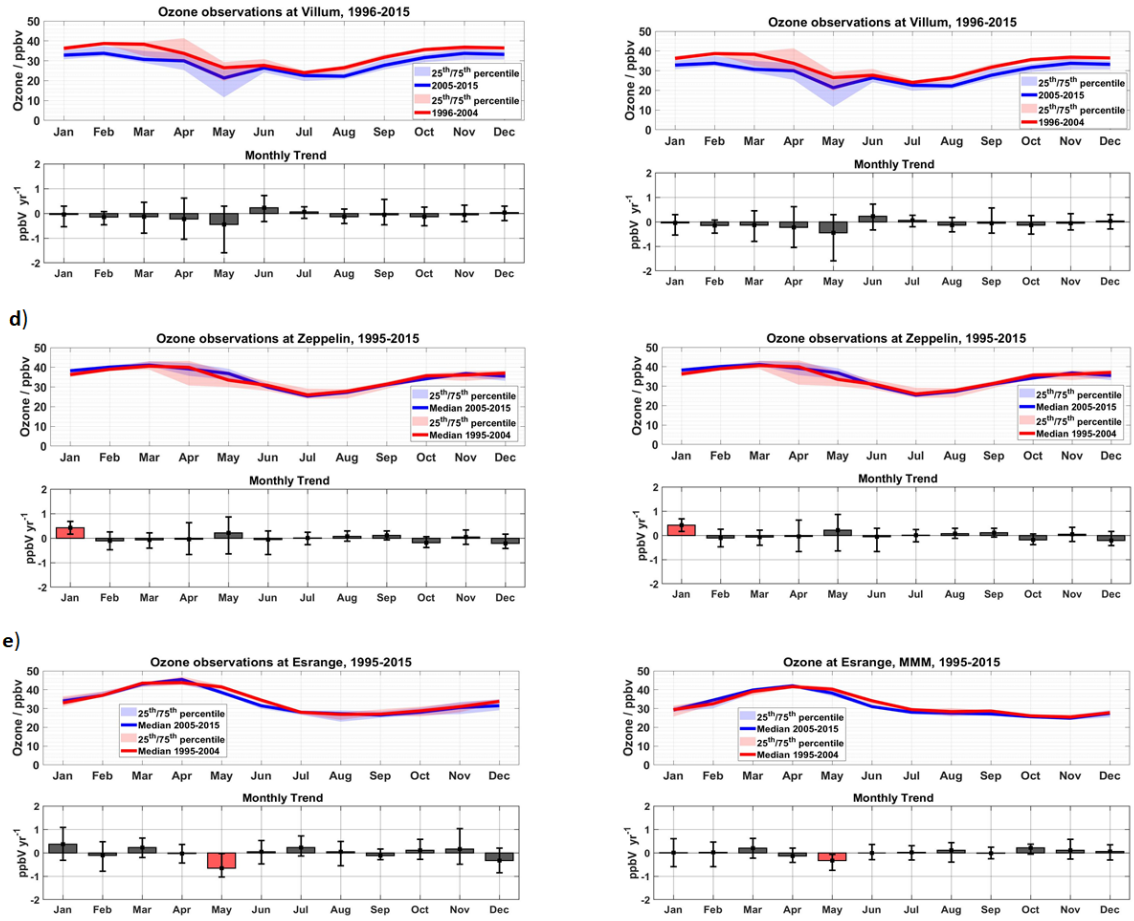


***Figure 3:*** *Comparison of observed (left) and MMM (right) surface $O_3$ trends and seasonal cycles at a) Alert, b) Utqiaġvik,* c) *Villum, d) Zeppelin, and e) Esrange. Upper panels: seasonal cycles for 1995-2004 (red lines) vs 2005-2015 (blue lines). Shaded areas show upper and lower quartiles of monthly values (observations only). Lower panels: monthly median trends in ppbv per year for 1995-2015, or shorter periods depending on data availability. Box coloring and error bars are the same as Fig. 2.*

# 4 Arctic ozone trends in the free troposphere

## 4.1 Observed vertical trends

This analysis focuses on $O_3$ changes in the lower and mid-troposphere. Figure 4 shows observed relative trends at six Arctic ozonesonde sites from 925-400 hPa for 1993-2019. Absolute trends above and below 400 hPa, and relative trends from 925-100 hPa, are also calculated (Figs. S7a,

S7b). Overall, while there are few ss trends, there seems to be a "dipole effect" with positive trends in winter and summer, and negative trends in spring and autumn. Positive ss winter (Jan/Dec) trends are found up to 400 hPa at most sites (except Resolute), and also at Scoresbysund in early spring. Positive wintertime trends are more evident in the earlier period in the upper troposphere (UT) and lower stratosphere (LS) (Fig. S8). Eureka, Resolute, and Sodankyla have periods with negative trends especially during spring and early summer in the lower troposphere. Resolute decreases extend up to 500 hPa in March-April. Relative ss trends vary from -1.5% to +0.5-1.0 % per year (Figs. 4, S7b) while stronger negative trends are diagnosed in later years (1999-2019) compared to 1993-2013 at all sites (Fig. S8).

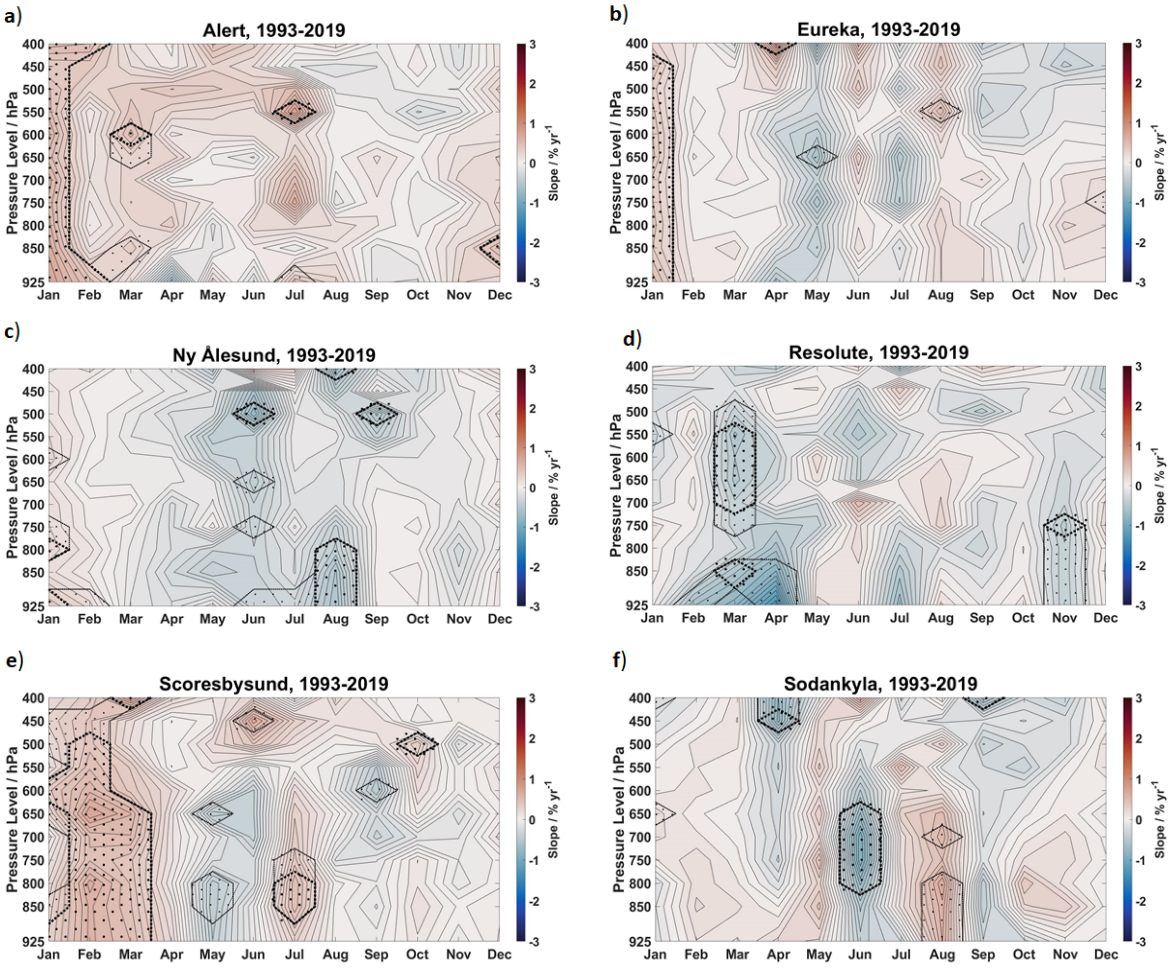


***Figure 4:*** *Vertical trends in observed monthly $O_3$ for 1993-2019, relative to monthly median concentrations, in % per year, from 925-400 hPa at a) Alert, b) Eureka, c) Ny Alesund, d) Resolute, e) Scoresbysund, and f) Sodankyla. Stippled lines/areas show statistical significance at the 90$^{th}$ % CL (smaller marker size) and 95$^{th}$ % CL (larger marker size).*

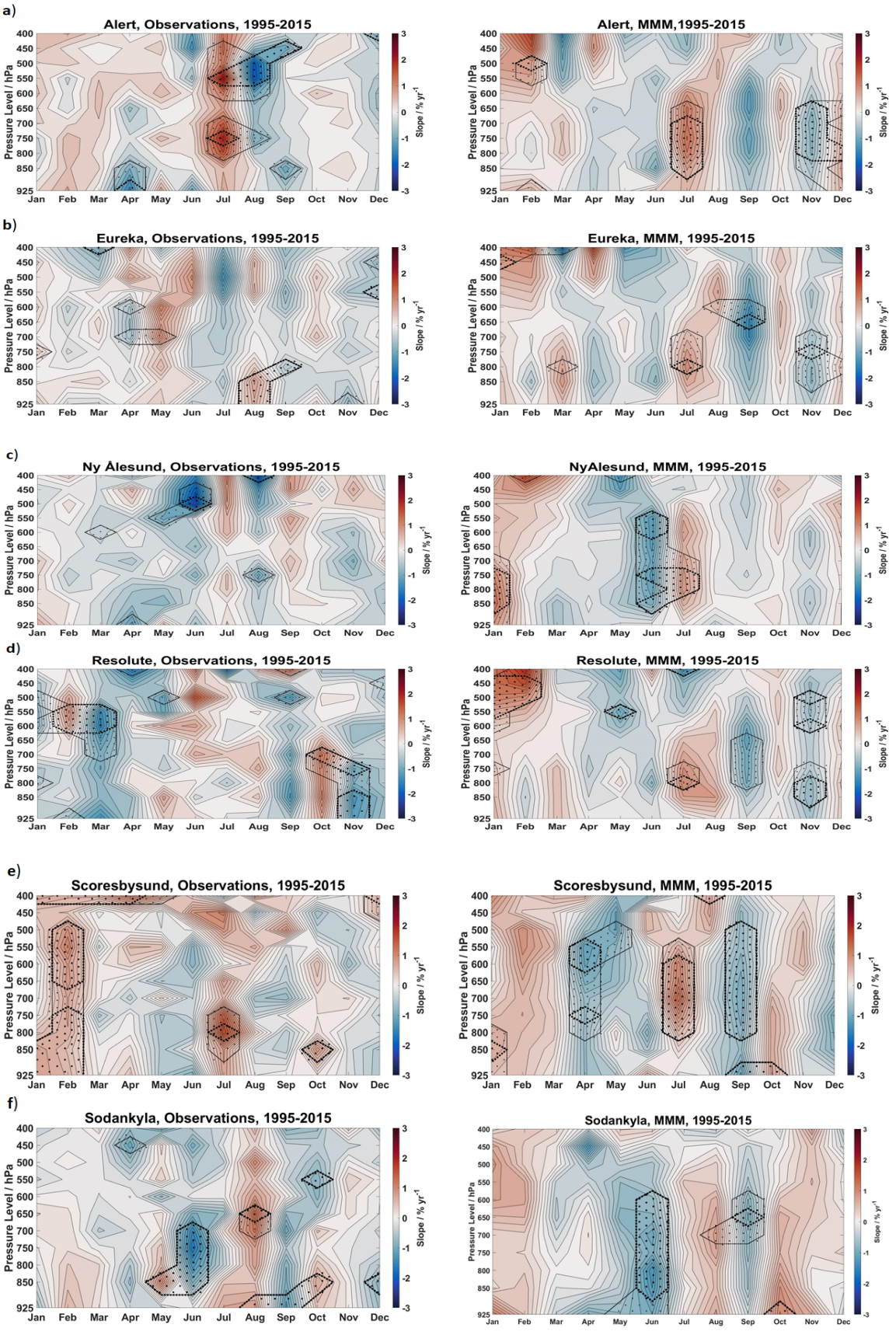
a)
Alert, Observations, 1995-2015
Alert, MMM,1995-2015
b)
Eureka, Observations, 1995-2015
Eureka, MMM, 1995-2015
c)
Ny Ålesund, Observations, 1995-2015
NyAlesund, MMM, 1995-2015
d)
Resolute, Observations, 1995-2015
Resolute, MMM, 1995-2015
e)
Scoresbysund, Observations, 1995-2015
Scoresbysund, MMM, 1995-2015
f)
Sodankyla, Observations, 1995-2015
Sodankyla, MMM, 1995-2015
Pressure Level / hPa
Slope / % yr-1
Jan Feb Mar Apr May Jun Jul Aug Sep Oct Nov Dec

***Figure 5:*** *Comparison of observed (left) and MMM (right) vertical trends in monthly $O_3$, relative to monthly medians, in % per year, from 925-400 hPa over 1995-2015 at a) Alert, b) Eureka, c) Ny Alesund, d) Resolute, e) Scoresbysund, and f) Sodankyla. Shading/symbols are as in Fig. 4.*

### 4.2 Comparison of observed and modeled vertical trends

Figure 5 shows observed ozonesonde and MMM trends for 1995-2015 up to 400 hPa (see Fig. S9 for results up to 100 hPa). Only results from 5 models are used, since EMEP MSC-W only provided surface $O_3$. The MMMs appear to capture the observed "dipole effect" seen in the observed trends. Models also capture observed increases in the winter but trends are overestimated at most sites, especially Ny Alesund and Sodankyla. Negative winter trends at Resolute are not simulated. This may be linked to positive modeled trends above 500 hPa at all sites (Fig. S9). Summertime positive ss MMM trends are larger than observed trends at some sites, e.g. Resolute and Ny Alesund.

## 5 Discussion and conclusions

Increasing annual surface $O_3$ trends at Arctic coastal sites, and at Zeppelin, are in qualitative agreement with Cooper et al. (2020), but in contrast to negative or non-significant surface trends at Canadian ozonesonde sites (Tarasick et al., 2016). A notable finding is that ss positive trends occur mainly in the winter months. While such increases were reported previously at Utqiaġvik (Gaudel et al. 2018; Christiansen et al., 2022) and Alert (Sharma et al., 2019), we confirm this tendency over the wider Arctic. Emission reductions of $NO_x$ in Europe and North America, and more recently over eastern Asia, have led to increasing wintertime $O_3$ at mid-latitudes due to less NO titration of $O_3$ (Jhun et al., 2015, Wang et al., 2022b, Bowman et al., 2022). This can explain observed increases in wintertime surface Arctic $O_3$, influenced primarily by transport of air masses from Europe (Hirdman et al., 2010). Evidence for declining $O_3$ precursor trends is supported by decreases in observed CO in the Arctic during autumn and winter (Fig. S10). At the same time, $CH_4$ continues to increase globally contributing to rising $O_3$ in the NH (Zeng et al., 2022) (see also Text S4 on Arctic $O_3$ precursor trends).

Another intriguing finding is springtime ss surface $O_3$ increases at Utqiaġvik (especially over 1999-2019, Fig S4), but no ss changes at Alert and Villum. Changes in $O_3$ concentrations at this

time of year may be driven by changes in ODE frequency linked to climate change or weather patterns (Oltmans et al, 2012). ODEs lead to zero or very low springtime $O_3$ due to bromine released from frost flowers or blowing snow (on sea-ice) (Simpson et al., 2007) or iodine compounds with a possible oceanic source (Benevant et al., 2022). Increases in springtime tropospheric bromine oxide have been observed from satellites, especially along the north coast of Greenland and central Arctic Ocean, correlating weakly with an increasing frequency in first year sea-ice (Bougoudis et al., 2020). Indeed, the frequency of low springtime $O_3$ concentrations has been increasing at Canadian high Arctic sites (see Fig. S11) but no ss springtime monthly trends are determined at Alert or Villum in our analysis. Springtime increases at Utqiaġvik could be due to stronger transport from mid-latitudes to this site during periods with a more northerly extension of the Pacific storm track, hampering conditions for ODEs (Koo et al., 2012). They could also be due to an increasing influence from local emissions, such as shipping or Alaskan petroleum extraction, when photochemistry becomes active in spring (Gunsch et al., 2017).

Decreases in springtime/early summer $O_3$ in northern Scandinavia, especially over the later 1999-2019 period, are consistent with negative trends reported at Tustervatn (Cooper et al., 2020), and sites in northern Sweden during summer (Andersson et al., 2017). These decreases are associated with lower maximum $O_3$ concentrations linked to reductions in European precursor emissions leading to less photochemical $O_3$ production (Cooper et al., 2020) although no ss trends in observed Arctic CO are found at this time of year (Fig. S10). Springtime ss negative trends at Summit may also be due to emission reductions over North America. Our results do not suggest a shift in the $O_3$ seasonal cycle toward higher concentrations in the spring (i.e. moving back toward pre-industrial $O_3$ seasonality) as reported at NH mid-latitudes (Bowman et al., 2022). Another explanation for decreasing springtime $O_3$ at the surface could be that reductions in snow cover (Mudryk et al., 2020) are leading to more $O_3$ dry deposition to Scandinavian forests.

The observed and modeled surface trend comparison covers 1995-2015, thereby missing the later time period when stronger observed $O_3$ trends are found, especially ss positive trends in winter. MMMs capture wintertime $O_3$ increases at Zeppelin, but overestimate at Alert and miss increase at Utqiaġvik. However, Whaley et al. (2023) noted that these models underestimate wintertime Arctic $O_3$ due to deficiencies modeling shallow boundary layers, $O_3$ deposition or $NO_x$ lifetimes.

Nevertheless, decreasing winter trends in surface CO are captured at Alert and Utqiaġvik (Fig. S10). Ss positive spring $O_3$ trend at Utqiaġvik is not evident in MMM trends over 1995-2015. However, the models do not capture springtime $O_3$ seasonality due to incorrect simulation of transport patterns (Oltmans et al., 2012) or missing surface halogen chemistry (Whaley et al., 2023). Negative ss springtime (May) trends are not always reproduced, possibly reflecting issues in the emission trends or modeled dry deposition.

FT $O_3$ trends are ss positive in winter at all Arctic sites, except Resolute, in common with several coastal Arctic surface sites. These results are in-line with increases reported at NH mid-latitudes (Cooper et al., 2020), and at Canadian ozonesonde sites (up to 400 hPa), except Resolute (Wang et al., 2022a). MMM trends are similar to observed trends over 1995-2015, including where they are ss. Patterns in observed trends are quite well captured, notably positive ss trends in winter and summer, although they tend to be overestimated. Observed negative trends in spring, extending from near the surface into the FT, are generally reproduced, and are likely to be due to decreasing $NO_x$ emissions leading to lower FT $O_3$ where photochemical production is $NO_x$-limited. Overestimation of winter trends contrasts to previous studies where models underestimated NH trends (Wang et al., 2022a; Christiansen et al., 2022). This may be due to differences in model transport or $O_3$ precursor emission trends, including $NO_x$ reductions (see also Text S4). AMAP models overestimate mid-latitude FT $O_3$ (Whaley et al., 2023), possibly suggesting a larger sensitivity to precursor emission changes.

Observed trends in the UT (LS) appear to have switched from positive to negative since 1993 in winter/spring, which may explain stronger positive FT trends in the earlier part of the record (1993-2013). More frequent positive phases of the Arctic Oscillation in recent years may be contributing with a weaker Brewer-Dobson circulation leading to less transport of stratospheric $O_3$ into the Arctic UT-LS, a higher tropopause height, and thus lower $O_3$ concentrations in this region (Zhang et al., 2017). However, Liu et al. (2020) did not detect any trend in the stratospheric $O_3$ flux into the Arctic UT. On the other hand, Wang et al. (2022a) attributed FT increases in NH mid-high latitude $O_3$ to increases in aircraft $NO_x$ emissions.

Overall, this study finds significant robust trends in Arctic tropospheric $O_3$. Observed trends are generally quite well captured by multi-model median results, although for example, they

overestimate wintertime free tropospheric increases, and miss Alaskan surface increases in spring. Further investigation into the causes of observed trends, and model performance, are needed taking into account uncertainties in the observations and models (Young et al., 2018; Fiore et al., 2022).

# Acknowledgements

We thank colleagues involved in AMAP (2021), notably K. von Salzen (Env. Canada), M. Flanner (U. Michigan). Technicians and logistical support staff are gratefully acknowledged for their work on data collection: D. Worthy (Alert), K. Sjöberg (Esrange), K. Saarnio (Pallas), B. Jensen, C. Christoffersen, K. Mortensen (Villum), and B. Thomas (Utqiaġvik/Barrow). None of the authors declare any real or perceived financial conflicts of interests. Multiple funders are acknowledged for support (see author metadata).

# Data Availability Statement:

Surface $O_3$ monitoring datasets are provided by EMEP (European Monitoring and Evaluation Program), and Global Atmosphere Watch (GAW) World Data Centre for Reactive Gases. EMEP and GAW $O_3$ data are available via the EBAS data portal (from end of 1989 to present). CO data at Utqiaġvik/Barrow and Zeppelin are also available via the EBAS data portal: http://ebas.nilu.no. Select the station name, and the component (CO, $O_3$) to access the data files. Canadian surface $O_3$ data can be downloaded from: https://data-donnees.ec.gc.ca/data/air/monitor/networks-and-studies/alert-nunavut-ground-level-ozone-study/. Canadian surface CO is available at: https://data-donnees.ec.gc.ca/data/air/monitor/national-air-pollution-surveillance-naps-program/?lang=en. Click on folders Data, Year, ContinuousData, then HourlyData. Surface $O_3$ records for Utqiaġvik/Barrow (BRW) and Summit (SUM) are provided by PE and IE via NOAA GML. Data is available at https://gml.noaa.gov/aftp/data/ozwv/SurfaceOzone/. Click on the directories for BRM or SUM to obtain the data. Surface $O_3$ measurements at Summit are made possible via the U.S. National Science Foundation Office of Polar Programs and their contract with Battelle Arctic Research Operations (contract #49100420C0001). Ny Ålesund, Scoresbysund and Sodankylä ozonesonde data are obtained as part of the Network for the Detection of Atmospheric

Composition Change (NDACC). Data is available via https://ndacc.larc.nasa.gov/index.php/stations. Click on the relevant site location to access the data files. Ozonesonde data for Alert, Resolute and Eureka have been reprocessed according to Tarasick et al. (2016), available at https://hegiftom.meteo.be/datasets/ozonesondes.

All model output files in NetCDF format from the simulations used in this study can be found here: https://open.canada.ca/data/en/dataset/c9a333ea-b81c-4df3-9880-ea7c3daeb76f. Model codes for GISS-E2.1 are available at: https://www.giss.nasa.gov/tools/modelE/.

Open-source codes for the Mann-Kendall test associated with Sen's slope are distributed under the BSD 3-Clause License in dedicated GitHub repositories hosted within the "mannkendall" organization (https://github.com/mannkendall), a Matlab (Collaud Coen and Vogt, 2020, https://doi.org/10.5281/zenodo.4134618, https://github.com/mannkendall/Matlab), Python (Vogt, 2020, https://doi.org/10.5281/zenodo.4134435, https://github.com/mannkendall/Python), and R (Bigi and Vogt, 2020, https://doi.org/10.5281/zenodo.4134632, https://github.com/mannkendall/R). Last access for all codes 27 January 2023.

# References

AMAP. (2015). AMAP Assessment 2015: Black carbon and ozone as Arctic climate forcers. *Arctic Monitoring and Assessment Programme (AMAP)*, 116, ISBN 978-82-7971-092-9. https://www.amap.no/documents/doc/amap-assessment-2015-black-carbon-and-ozone-as-arctic-climate-forcers/1299

AMAP (2021). AMAP Assessment 2021: Impacts of short-lived climate forcers on Arctic climate, air quality, and human health. Arctic Monitoring and Assessment Programme (AMAP), Tromsø, Norway, in press, 2023. Last access 24 January 2023. https://www.amap.no/documents/doc/amap-assessment-2021-impacts-of-short-lived-climate-forcers-on-arctic-climate-air-quality-and-human-health/3614

Andersson, C., Alpfjord, H., Robertson, L., Karlsson, P. E., & Engardt, M. (2017) Reanalysis of and attribution to near-surface ozone concentrations in Sweden during 1990–2013, *Atmospheric Chemistry and Physics, 17*, 13869–13890, https://doi.org/10.5194/acp-17-13869-2017.

Anenberg, S. C., Horowitz, L. W., Tong, D. Q., & West, J. J. (2010). An estimate of the global burden of anthropogenic ozone and fine particulate matter on premature human mortality using atmospheric modeling. *Environmental Health Perspectives*, *118*(9), 1189–1195. https://doi.org/10.1289/ehp.0901220

371 Arnold, S. R., Lombardozzi, D., Lamarque, J.-F., Richardson, T., Emmons, L. K., Tilmes, S., et al.
372 (2018). Simulated global climate response to tropospheric ozone-induced changes in plant
373 transpiration. *Geophysical Research Letters*, *45*(23), 13070–13079.
374 https://doi.org/10.1029/2018GL079938

375 Bahramvash Shams, S., Walden, V. P., Petropavlovskikh, I., Tarasick, D., Kivi, R., Oltmans, et al. (2019)
376 Variations in the vertical profile of ozone at four high-latitude Arctic sites from 2005 to 2017,
377 *Atmospheric Chemistry and Physics, 19*, 9733–9751, https://doi.org/10.5194/acp-19-9733-2019

378 Barrie, L., Bottenheim, J., Schnell, R. et al. (1988) Ozone destruction and photochemical reactions at
379 polar sunrise in the lower Arctic atmosphere. *Nature, 334***,** 138–141.
380 https://doi.org/10.1038/334138a0

381 Benavent, N., Mahajan, A. S., Li, Q., Cuevas, C. A., Schmale, J., Angot, H., et al. (2022). Substantial
382 contribution of iodine to Arctic ozone destruction. *Nature Geoscience*, 15(10), 770–773.
383 https://doi.org/10.1038/s41561-022-01018-w

384 Bougoudis, I., Blechschmidt, A.-M., Richter, A., Seo, S., Burrows, J. P., Theys, N., & Rinke, A. (2020).
385 Long-term time series of Arctic tropospheric BrO derived from UV–VIS satellite remote sensing and
386 its relation to first-year sea ice. *Atmospheric Chemistry and Physics*, 20(20), 11869–11892.
387 https://doi.org/10.5194/acp-20-11869-2020

388 Bowman, H., Turnock, S., Bauer, S. E., Tsigaridis, K., Deushi, M., Oshima, N., et al. (2022). Changes in
389 anthropogenic precursor emissions drive shifts in the ozone seasonal cycle throughout the northern
390 midlatitude troposphere. *Atmospheric Chemistry and Physics*, 22(5), 3507–3524.
391 https://doi.org/10.5194/acp-22-3507-2022

392 Christiansen, A., Mickley, L. J., Liu, J., Oman, L. D., & Hu, L. (2022). Multidecadal increases in global
393 tropospheric ozone derived from ozonesonde and surface site observations: can models reproduce
394 ozone trends? *Atmospheric Chemistry and Physics*, 22(22), 14751–14782.
395 https://doi.org/10.5194/acp-22-14751-2022

396 Christiansen, B., Jepsen, N., Kivi, R., Hansen, G., Larsen, N., and Korsholm, U. S. (2017) Trends and
397 annual cycles in soundings of Arctic tropospheric ozone, *Atmospheric Chemistry and Physics,* 17,
398 9347–9364. https://doi.org/10.5194/acp-17-9347-2017

399 Clifton, O. E., Fiore, A. M., Massman, W. J., Baublitz, C. B., Coyle, M., Emberson, L., et al. (2020). Dry
400 deposition of ozone over land: Processes, measurement, and modeling. *Reviews of Geophysics*,
401 *58*(1). https://doi.org/e2019RG000670

402 Collaud Coen, M., Andrews, E., Bigi, A., Martucci, G., Romanens, G., Vogt, F. P. A., and Vuilleumier,
403 L. (2020) Effects of the prewhitening method, the time granularity, and the time segmentation on the
404 Mann–Kendall trend detection and the associated Sen's slope, *Atmospheric Measurement*
405 *Techniques, 13*, 6945-6964. https://doi/org/10.5194/amt-13-6945-2020

406 Cooper, O. R., Schultz, M. G., Schröder, S., Chang, K.-L., Gaudel, A., Benítez, G. C., et al. (2020).
407 Multi-decadal surface ozone trends at globally distributed remote locations. *Elementa: Science of the*
408 *Anthropocene*, *8*, 23. https://doi.org/10.1525/elementa.420

409 Dibb, J. E. (2007). Vertical mixing above Summit, Greenland: Insights into seasonal and high frequency
410 variability from the radionuclide tracers 7Be and 210Pb. *Atmospheric Environment*, 41(24), 5020–
411 5030. https://doi.org/10.1016/j.atmosenv.2006.12.005

412 Fiore, A. M., Hancock, S. E., Lamarque, J.-F., Correa, G. P., Chang, K.-L., Ru, M., et al. (2022).
413 Understanding recent tropospheric ozone trends in the context of large internal variability: a new
414 perspective from chemistry-climate model ensembles. *Environmental Research: Climate*, 1(2),
415 025008. https://doi.org/10.1088/2752-5295/ac9cc2

416 Gaudel, A., Cooper, O. R., Ancellet, G., Barret, B., Boynard, A., Burrows, J. P., et al. (2018).
417 Tropospheric Ozone Assessment Report: Present-day distribution and trends of tropospheric ozone
418 relevant to climate and global atmospheric chemistry model evaluation. *Elementa: Science of the*
419 *Anthropocene*, *6*, 39. https://doi.org/10.1525/elementa.291

420 Griffiths, P. T., Murray, L. T., Zeng, G., Shin, Y. M., Abraham, N. L., Archibald, A. T., et al. (2021).
421 Tropospheric ozone in CMIP6 simulations. *Atmospheric Chemistry and Physics, 21(5),* 4187–4218.
422 https://doi.org/10.5194/acp-21-4187-2021

423 Gunsch, M. J., Kirpes, R. M., Kolesar, K. R., Barrett, T. E., China, S., Sheesley, R. J., et al. (2017).
424 Contributions of transported Prudhoe Bay oil field emissions to the aerosol population in Utqiaġvik,
425 Alaska. *Atmospheric Chemistry and Physics, 17(17)*, 10879–10892. https://doi.org/10.5194/acp-17-
426 10879-2017

427 Hirdman, D., Sodemann, H., Eckhardt, S., Burkhart, J. F., Jefferson, A., Mefford, T., et al. (2010). Source
428 identification of short-lived air pollutants in the Arctic using statistical analysis of measurement data
429 and particle dispersion model output. *Atmospheric Chemistry and Physics*, 10(2), 669–693.
430 https://doi.org/10.5194/acp-10-669-2010

431 Jhun, I., Coull, B. A., Zanobetti, A., & Koutrakis, P. (2015). The impact of nitrogen oxides concentration
432 decreases on ozone trends in the USA. *Air Quality, Atmosphere and Health*, 8(3), 283–292.
433 https://doi.org/10.1007/s11869-014-0279-2

434 Koo, J. H., Wang, Y., Kurosu, T. P., Chance, K., Rozanov, A., Richter, A., et al. (2012) Characteristics of
435 tropospheric ozone depletion events in the Arctic spring: analysis of the ARCTAS, ARCPAC, and
436 ARCIONS measurements and satellite BrO observations. *Atmospheric Chemistry and Physics*,
437 12(20), 9909–9922. https://doi.org/10.5194/acp-12-9909-2012

438 Law, K. S., Stohl, A., Quinn, P. K., Brock, C. A., Burkhart, J. F., Paris, J.-D., et al. (2014). Arctic air
439 pollution: New insights from POLARCAT-IPY. *Bulletin of the American Meteorological Society*,
440 95(12), 1873–1895. https://doi.org/10.1175/bams-d-13-00017.1

441 Liu, J., Rodriguez, J. M., Oman, L. D., Douglass, A. R., Olsen, M. A., & Hu, L. (2020). Stratospheric
442 impact on the Northern Hemisphere winter and spring ozone interannual variability in the
443 troposphere. *Atmospheric Chemistry and Physics*, *20*(11), 6417–6433. https://doi.org/10.5194/acp-
444 20-6417-2020

445 Mudryk, L., Santolaria-Otín, M., Krinner, G., Ménégoz, M., Derksen, C., Brutel-Vuilmet, C., et al.
446 (2020). Historical Northern Hemisphere snow cover trends and projected changes in the CMIP6
447 multi-model ensemble. *The Cryosphere*, 14(7), 2495–2514. https://doi.org/10.5194/tc-14-2495-2020

448 Oltmans, S. J., Johnson, B. J., & Harris, J. M. (2012) Springtime boundary layer ozone depletion at
449 Barrow, Alaska: Meteorological influence, year-to-year variation, and long-term change, *Journal of*
450 *Geophysical Research,* 117, D00R18, https://doi.org/10.1029/2011JD016889

451 Rap, A., Richards, N. A. D., Forster, P. M., Monks, S. A., Arnold, S. R., and Chipperfield, M. P. (2015).
452 Satellite constraint on the tropospheric ozone radiative effect. *Geophysical Research Letters*, *42*(12),
453 5074–5081. https://doi.org/10.1002/2015GL064037

454 Sand, M., Berntsen, T. K., von Salzen, K., Flanner, M. G., Langner, J., & Victor, D. G. (2016). Response
455 of Arctic temperature to changes in emissions of short-lived climate forcers. *Nature Climate*
456 *Change*, 6(3), 286–289. https://doi.org/10.1038/nclimate2880

457 Schmale, J., Arnold, S. R., Law, K. S., Thorp, T., Anenberg, S., Simpson, W. R., Mao, J., and Pratt, K. A.
458 (2018) Local Arctic air pollution: A neglected but serious problem, *Earth's Future*, 6, 1385-1412.
459 https://doi.org/10.1029/2018ef000952

460 Schmeisser, L., Backman, J., Ogren, J. A., Andrews, E., Asmi, E., Starkweather, S., et al. (2018).
461 Seasonality of aerosol optical properties in the Arctic. *Atmospheric Chemistry and Physics*, 18(16),
462 11599–11622. https://doi.org/10.5194/acp-18-11599-2018

463 Sen, P. K. (1968), Estimates of the regression coefficient based on Kendall's Tau, *Journal of the*
464 *American Statistical Association, 63*, 1379-1389. https://doi.org/10.1080/01621459.1968.10480934

465 Sharma, S., L. A. Barrie, E. Magnusson, G. Brattstrom, W. R. Leaitch, A. Steffen and S. Landsberger
466 (2019) A factor and trends analysis of multidecadal lower tropospheric observations of Arctic
467 Aerosol Composition, Black Carbon, Ozone, and Mercury at Alert, Canada. *Journal of Geophysical*
468 *Research-Atmospheres, 124*(24): 14133-14161. https://doi.org/10.1029/2019JD030844

469 Simpson, W. R., von Glasow, R., Riedel, K., Anderson, P., Ariya, P., Bottenheim, J., et al. (2007).
470 Halogens and their role in polar boundary-layer ozone depletion. *Atmospheric Chemistry and*
471 *Physics*, *7*(16), 4375–4418. https://doi.org/10.5194/acp-7-4375-2007

472 Tarasick, D. W., Davies, J., Smit, H. G. J., & Oltmans, S. J. (2016). A re-evaluated Canadian ozonesonde
473 record: measurements of the vertical distribution of ozone over Canada from 1966 to 2013.
474 *Atmospheric Measurement Techniques*, *9*(1), 195–214. https://doi.org/10.5194/amt-9-195-2016

475 Tarasick, D., Galbally, I.E., Cooper, O.R., Schultz, M.G., Ancellet, G., Leblanc, et al. (2019).
476 Tropospheric Ozone Assessment Report: Tropospheric ozone from 1877 to 2016, observed levels,

trends and uncertainties. *Elementa: Science of the Anthropocene, 7*: 39. https://doi.org/10.1525/elementa.376

Theil, H. (1950) A rank-invariant method of linear and polynomial regression analysis, *Nederl. Akad. Wetensch., Proc., 53*, 386--392, https://ir.cwi.nl/pub/18446

Turnock, S. T., Allen, R. J., Andrews, M., Bauer, S. E., Deushi, M., Emmons, L., et al. (2020). Historical and future changes in air pollutants from CMIP6 models. *Atmospheric Chemistry and Physics*, 20(23), 14547–14579. https://doi.org/10.5194/acp-20-14547-2020

von Salzen, K., Whaley, C. H., Anenberg, S. C., Van Dingenen, R., Klimont, Z., Flanner, M. G., et al. (2022). Clean air policies are key for successfully mitigating Arctic warming. *Communications Earth & Environment*, 3(1), 222. https://doi.org/10.1038/s43247-022-00555-x

Wang, H., X. Lu, D. J. Jacob, O. R. Cooper, K.-L. Chang, K. Li, et al. (2022a) Global tropospheric ozone trends, attributions, and radiative impacts in 1995-2017: an integrated analysis using aircraft (IAGOS) observations, ozonesonde, and multi-decadal chemical model simulations, *Atmospheric Chemistry and Physics*, *22,* 13753-13782. https://doi.org/10.5194/acp-22-13753-2022

Wang, T, L. Xue, Z. Feng, J. Dai, Y. Zhang, & Y. Tan (2022b) *Environmental Research Letters,* 17**,** 063003, Ground-level ozone pollution in China: a synthesis of recent findings on influencing factors and impacts. https://doi.org/10.1088/1748-9326/ac69fe

Whaley, C. H., Mahmood, R., von Salzen, K., Winter, B., Eckhardt, S., Arnold, et al. (2022), Model evaluation of short-lived climate forcers for the Arctic Monitoring and Assessment Programme: a multi-species, multi-model study, *Atmospheric Chemistry and Physics, 22*, 5775–5828. https://doi.org/10.5194/acp-22-5775-2022

Whaley, C. H., Law, K. S., Hjorth, J. L., Skov, H., Arnold, S. R., Langner, J., Pernov, et al. (2023), Arctic tropospheric ozone: assessment of current knowledge and model performance. *Atmospheric Chemistry and Physics*, 23, 637-661. https://doi.org/10.5194/acp-23-637-2023

Young, P.J., V. Naik, A. M. Fiore, A. Gaudel, J. Guo‖, M. Y. Lin, et al. (2018) Tropospheric Ozone Assessment Report: Assessment of global-scale model performance for global and regional ozone distributions, variability, and trends. *Elementa: Science of the Anthropocene*, 6: 10. https://doi.org/10.1525/elementa.265

Zeng, G., Morgenstern, O., Williams, J. H. T., O'Connor, F. M., Griffiths, P. T., Keeble, J., et al. (2022). Attribution of stratospheric and tropospheric ozone changes between 1850 and 2014 in CMIP6 models. *Journal of Geophysical Research: Atmospheres*, 127. https://doi.org/10.1029/2022JD036452

Zhang, J., F. Xie, W. Tian, Y. Han, K. Zhang, Y. Qi et al. (2017) Influence of the Arctic Oscillation on the vertical distribution of wintertime ozone in the stratosphere and upper troposphere over the Northern Hemisphere, *Journal of Climate*, 30(8). https://doi.org/10.1175/JCLI-D-16-0651.1

# Arctic Tropospheric Ozone Trends

K. S. Law[1], J. Liengaard Hjorth[2], J. B. Pernov[2,3], C. H. Whaley[4], H. Skov[2], M. Collaud Coen[5], J. Langner[6], S. R. Arnold[7], D. Tarasick[8], J. Christensen[2], M. Deushi[9], P. Effertz[10,14], G. Faluvegi[11,12], M. Gauss[13], U. Im[2], N. Oshima[9], I. Petropavlovskikh[10,14], D. Plummer[4], K. Tsigaridis[11,12], S. Tsyro[13], S. Solberg[15] and S.T. Turnock[16,7]

[1]Sorbonne Université, LATMOS-IPSL, UVSQ, CNRS, Paris, France
[2]Department of Environmental Science, Interdisciplinary Centre for Climate Change, Aarhus University, Frederiksborgvej 4000, Roskilde, Denmark
[3]Extreme Environments Research Laboratory, École Polytechnique Fédérale de Lausanne, 1951 Sion, Switzerland
[4]Canadian Centre for Climate modeling and analysis, Environment and Climate Change Canada, Victoria, BC, Canada
[5]Federal Office of Meteorology and Climatology, MeteoSwiss, Payerne, Switzerland
[6]Swedish Meteorological and Hydrological Institute, Norrköping, Sweden
[7]Institute for Climate and Atmospheric Science, School of Earth and Environment, University of Leeds, Leeds, United Kingdom
[8]Air Quality Research Division, Environment and Climate Change Canada, Toronto, ON, Canada
[9]Meteorological Research Institute, Japan Meteorological Agency, Tsukuba, Japan
[10]Cooperative Institute for Research in Environmental Sciences (CIRES), University of Colorado, Boulder, CO, USA.
[11]NASA Goddard Institute for Space Studies, New York, NY, USA
[12]Center for Climate Systems Research, Columbia University; New York, USA
[13]Norwegian Meteorological Institute, Oslo, Norway
[14]National Oceanic and Atmospheric Administration (NOAA) ESRL Global Monitoring Laboratory, Boulder, CO, USA.
[15]Norwegian Institute for Air Research (NILU), Kjeller, Norway.
[16]Met Office Hadley Centre, Exeter, UK

Corresponding author: Kathy.Law@latmos.ipsl.fr

## Key Points:

- Coherent ozone trend analysis methodology applied to multi-decade, pan-Arctic surface and ozonesonde datasets and multi-model medians.
- Increasing winter Arctic tropospheric ozone overestimated by models in the free troposphere, Alaskan spring surface increases not captured.
- Spring (summer) decreases (increases) in observed ozone throughout the troposphere, not always simulated by models.

# Abstract

Trends in tropospheric ozone, an important air pollutant and short-lived climate forcer (SLCF), are estimated using available surface and ozonesonde profile data for 1993-2019. Using a coherent methodology, observed trends are compared to modeled trends (1995-2015) from the Arctic Monitoring Assessment Programme SLCF 2021 assessment. Statistically significant increases in observed surface ozone at Arctic coastal sites, notably during winter, and concurrent decreasing trends in surface carbon monoxide, are generally captured by multi-model median (MMM) trends. Wintertime increases are also estimated in the free troposphere at most Arctic sites, but tend to be overestimated by the MMMs. Springtime surface ozone increases in northern coastal Alaska are not simulated while negative springtime trends in northern Scandinavia are not always reproduced. Possible reasons for observed changes and model behavior are discussed, including decreasing precursor emissions, changing ozone sinks, and variability in large-scale meteorology.

**Plain Language Summary**

The Arctic is warming much faster than the rest of the globe due to increases in carbon dioxide, and other trace constituents like ozone, also an air pollutant. However, improved understanding is needed about long-term changes or trends in Arctic tropospheric ozone. A coherent methodology is applied to determine trends in surface and regular profile measurements over the last 20-30 years, and results from six chemistry-climate models. Statistically significant increases in observed ozone are found at the surface and in the free troposphere during winter in the high Arctic. Paradoxically, decreases in nitrogen oxide emissions at mid-latitudes appear to be leading to increases in ozone during winter, but associated increases in Arctic tropospheric ozone tend to be overestimated in the models. Increases are also found at the surface in northern Alaska during spring but not reproduced by the models. The causes are unknown but could be related to changes in local sources or sinks of Arctic ozone or in large-scale weather patterns. Declining mid-latitude emissions may also explain negative surface ozone trends over northern Scandinavia in spring that are not always captured by the models. Further work is needed to understand changes in Arctic tropospheric ozone.


# 1 Introduction

Tropospheric ozone ($O_3$) is a short-lived climate forcer (SLCF) contributing to global and Arctic warming (AMAP, 2015; Sand et al, 2016; von Salzen et al. 2022), and a critical secondary air pollutant, detrimental to human health (Anenberg et al., 2010) and ecosystems (Arnold et al., 2018). The Arctic tropospheric $O_3$ budget is complex, as recently discussed in a companion paper, Whaley et al. (2023). It originates from photochemical production of anthropogenic or

natural emissions of $O_3$ precursors, including nitrogen oxides ($NO_x$), carbon monoxide (CO) and methane ($CH_4$), in the Arctic, or following air mass transport from mid-latitudes, as well as transport of $O_3$ from the stratosphere (Law et al., 2014; Schmale et al., 2018). Sinks include photochemical destruction, including reactions involving halogens leading to so-called ozone depletion events (ODEs) (Barrie, et al., 1988; Simpson et al., 2007), and surface dry deposition (Clifton et al., 2020). Growth in anthropogenic emissions since pre-industrial times has led to increases in tropospheric $O_3$ throughout the Northern Hemisphere (NH) (Tarasick et al., 2019; Turnock et al., 2020; Cooper et al., 2020) contributing to observed global and Arctic warming over the past century (e.g. Griffiths et al., 2021). Since the mid-1990s, a mix of relatively weak positive and negative trends (+1 to -1 parts per billion by volume (ppbv) per decade) have been reported in the NH at the surface and in the free troposphere (FT), with largest increases over south and eastern Asia, associated with increasing anthropogenic emissions (Cooper et al., 2020; Wang et al., 2022a).

To date, only a few studies have focused on assessing tropospheric $O_3$ trends in the Arctic. While positive $O_3$ trends were diagnosed at several surface sites, results are not always statistically significant, and both positive and negative trends were reported at some Canadian sites (Tarasick et al., 2016; Sharma et al., 2019; Cooper et al., 2020). In the Arctic FT, studies found significant positive trends (Christiansen et al., 2017; Wang et al., 2022a), no trends (Tarasick et al., 2016), or mixed trends in different seasons (Bahramvash Shams et al., 2019). Differences in the periods analyzed, sign or magnitude of trends emphasizes the need to further examine trends using the same methodology. Coherent estimation of observed trends, and evaluation of modeled trends, is needed to better understand $O_3$ changes and impacts on Arctic climate that are sensitive to the altitude where $O_3$ perturbations occur (Rap et al., 2015). This study assesses annual and monthly trends, together with possible evolution in seasonal cycles, of Arctic tropospheric $O_3$ over the last 20-30 years. Observed changes are compared to results from atmospheric chemistry-climate models run as part of the recent Arctic Monitoring and Assessment Programme (AMAP) SLCF assessment (AMAP, 2021; Whaley et al., 2022; von Salzen et al., 2022). Results are discussed in light of possible changes in sources and sinks of Arctic tropospheric $O_3$.

# 2 Methods

## 2.1 Measurements

The location of surface and ozonesonde sites used in this study are displayed in Fig. 1, together with the Arctic Circle at 66.6°N, used to define the Arctic. Annual surface trends are shown in the table grouped into 1) high Arctic coastal sites (Alert, Utqiaġvik/Barrow, Villum), Zeppelin (situated at 474m on Svalbard) and Summit (high altitude (FT) site on Greenland (3211m), and 2) European continental sites within (Pallas, Esrange), and just south (Tustervatn) of the Arctic Circle.


| Site | Annual trend (%) | Significance level | Period |
|---|---|---|---|
| ***High Arctic:*** | | | |
| Alert | **0.29** | 95% | 1999-2019 |
| | **0.24** | 95% | 1993-2019 |
| Utqiagvik | 0.53 | <90% | 1999-2019 |
| | 0.26 | <90% | 1993-2019 |
| Villum | **1.98** | 95% | 1999-2019 |
| | 0.68 | 90% | 1996-2019 |
| Zeppelin | -0.19 | <90% | 1999-2019 |
| | **0.18** | 90% | 1993-2019 |
| Summit | -0.28 | <90% | 2001-2019 |
| ***European continental Arctic and near-Arctic:*** | | | |
| Esrange | 0.08 | <90% | 1999-2019 |
| | 0.00 | <90% | 1993-2019 |
| Pallas | **-0.30** | 90% | 1998-2019 |
| | **-0.40** | 90% | 1995-2019 |
| Tustervatn | **-0.52** | 99% | 1999-2019 |
| | -0.18 | >90% | 1994-2019 |

***Figure 1.*** *Left: Location of surface (bold) and ozonesonde (italic) sites and showing the Arctic Circle (66.55°N). Right: annual $O_3$ trends at surface sites in % per year (left column), the significance level (middle column), calculated over periods shown in the right column. Statistically significant trends (above 90% confidence level) are in bold. Geographical coordinates for all sites are provided in Whaley et al. (2023). See text for details.*

Surface observations are from EBAS Level 2 data, station owners for Villum before 2001, Canada's Open Government Portal for Alert, and National Oceanic and Atmospheric

Administration (NOAA) for Summit, and Barrow Atmospheric Observatory, Utqiaġvik (Utqiaġvik from now on). Ozonesonde data are from the World Ozone and Ultraviolet Radiation Data Centre (WOUDC) and Network for the Detection of Atmospheric Composition Change (NDACC). See also the Supplementary Information (Text S1, Figs. S1 and S2, including data coverage).

### 2.2 Trend analysis

Observed monthly and annual trends in surface $O_3$ concentrations at different sites are determined using the non-parametric Mann-Kendall test at the $90^{th}$ and $95^{th}$ confidence level (CL) and Sen's slope methodology (Theil, 1950; Sen, 1968) (see Text S2). Daily median data are sorted into different months and pre-whitened, due to the presence of autocorrelation, via the 3PW algorithm from Collaud Coen et al. (2020). Trends using ozonesonde profiles are calculated based on weekly medians for selected pressure levels. For the calculation of relative trends, data are normalized by division with median values and multiplied by 100.

### 2.3 Modeled trends

Modeled trends at the surface and different altitudes are calculated for 1995-2015 using results from four global chemistry-climate models (CMAM, GISS-E2.1, MRI-ESM2, UKESM1) and two chemistry-transport models (DEHM, EMEP MSC-W) run using the same ECLIPSEv6b anthropogenic emissions, and nudged with meteorological reanalyses as part of AMAP (2021). Details can be found in Whaley et al. (2022), Text S3 and Table S1. Simulated monthly mean $O_3$ volume mixing ratios from the model grid box containing the measurement location are used to compute multi-model medians (MMMs). For ozonesonde comparisons, modeled vertical profiles are interpolated onto the same vertical bins as the measurements before trends are computed.

## 3 Surface ozone trends in the Arctic

### 3.1 Observed ozone trends

Annual trends are calculated for 1993-2019, or for the longest period with sufficient data, for all the sites (see Fig. 1, Table S2).

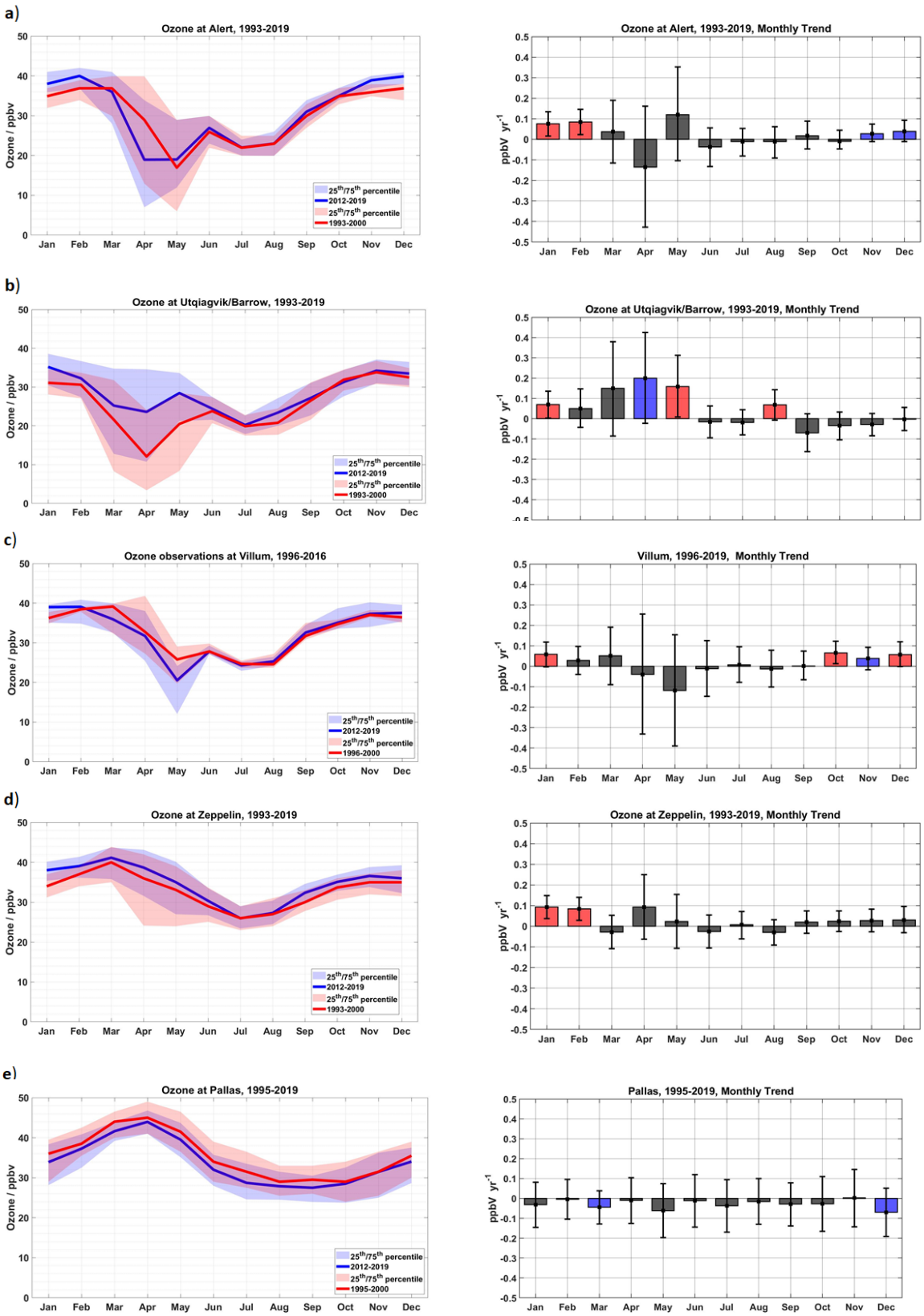
a)
Ozone at Alert, 1993-2019
Ozone / ppbv
25th/75th percentile
2012-2019
25th/75th percentile
1993-2000
Ozone at Alert, 1993-2019, Monthly Trend
ppbV yr-1
b)
Ozone at Utqiagvik/Barrow, 1993-2019
Ozone / ppbv
25th/75th percentile
2012-2019
25th/75th percentile
1993-2000
Ozone at Utqiagvik/Barrow, 1993-2019, Monthly Trend
ppbV yr-1
c)
Ozone observations at Villum, 1996-2016
Ozone / ppbv
25th/75th percentile
2012-2019
25th/75th percentile
1996-2000
Villum, 1996-2019, Monthly Trend
ppbV yr-1
d)
Ozone at Zeppelin, 1993-2019
Ozone / ppbv
25th/75th percentile
2012-2019
25th/75th percentile
1993-2000
Ozone at Zeppelin, 1993-2019, Monthly Trend
ppbV yr-1
e)
Ozone at Pallas, 1995-2019
Ozone / ppbv
25th/75th percentile
2012-2019
25th/75th percentile
1995-2000
Pallas, 1995-2019, Monthly Trend
ppbV yr-1
Jan Feb Mar Apr May Jun Jul Aug Sep Oct Nov Dec

***Figure 2.*** *Observed surface $O_3$ trends and seasonal cycles. Left: seasonal cycles of monthly median $O_3$ (ppbv) at a) Alert, b) Utqiaġvik, c) Villum, d) Zeppelin, and e) Pallas for 1993-2000 (blue lines) vs 2012-2019 (red lines). Shaded areas show upper and lower quartiles of hourly values. Right: monthly trends for 1993-2019. Boxes represent the slope of the trend in ppbv per year with red boxes significant at 95$^{th}$% CL, blue boxes at 90$^{th}$% CL, and black boxes not statistically significant. Error bars show 95$^{th}$% CLs. Results are shown for shorter periods depending on data availability.*

Average $O_3$ seasonal cycles are also calculated for earlier (1993-2000) and later (2012-2019) periods, to examine possible changes, together with monthly trends (Fig. 2) at selected sites (see Fig. S3 for other sites). Monthly trends are also analyzed for different 21-year periods (1993-2012, 1999-2019) (Fig. S4).

First considering high Arctic sites at coastal locations that exhibit a winter maximum with low spring concentrations attributed to ODEs, as discussed in Whaley et al. (2023). Alert has statistically significant ("ss") positive $O_3$ annual trends, as does Villum for the shorter time period 1999-2019, while annual trends at Utqiaġvik are not significant (see Fig. 1). Ss trends are also calculated in particular seasons, as shown in Fig. 2. Notably, ss positive trends are found during late autumn and/or winter at Alert, Villum and Utqiaġvik. Positive trends are also calculated for spring at Utqiaġvik (April-May). Winter trends at Alert and spring trends at Utqiaġvik are more pronounced when using the later record (1999-2019) (see Fig. S4). To further characterize these changes, probability distributions in observed $O_3$ concentrations are calculated for months with ss trends (see Fig. S5). Positive ss trends during winter and spring at Utqiaġvik are the result of a decrease (increase) in the frequency of low (high) concentrations (Jan.-May), whereas wintertime $O_3$ concentrations shifted recently towards higher values at Alert (Nov.-Feb.) and Villum (Oct.-Jan.). Zeppelin shows a different seasonal behavior compared to Arctic sea-level coastal sites with a spring maximum, more similar to remote mid-latitude sites. Here, ss positive annual trends are estimated for 1993-2019 (Fig. 1), and in winter (Fig. 2), driven by increases in the earlier part of the record (1993-2013) (Fig. S4).

Continental northern Scandinavian sites exhibit a different behavior with Pallas and Tustervatn showing ss negative annual trends but no ss annual (or monthly) trends at Esrange over any of the periods considered. The shape of the seasonal cycle for the earlier versus the later period is

similar at these sites, which also have a spring maximum like Zeppelin. $O_3$ appears to be decreasing throughout the year when comparing earlier and later periods although ss negative trends are only evident at Pallas (March, December), and at Tustervatn in spring and early summer (Fig. S4, 1999-2019 trends). Summit is more representative of the FT and samples air masses transported from North America and Asia, or of stratospheric origin (Dibb, 2007; Schmeisser et al., 2018). The annual trend, calculated over the shorter 2001-2019 record, is not ss at the 90$^{th}$ % CL, but ss negative monthly trends are estimated for January, March-May and September.

## 3.2 Comparison of observed and modeled surface trends

Figure 3 compares observed monthly and MMM trends for 1995-2015, or the closest possible time interval in case of years with missing observations. Results for other sites are shown in Fig. S6. Observed ss trends are more frequently diagnosed over 1993-2019 (Fig. 2) than over the shorter period ending in 2015 (Fig. 3). While the MMMs simulate $O_3$ seasonal cycles reasonably well, low $O_3$ concentrations are missed in spring, and wintertime $O_3$ is underestimated (Whaley et al., 2023). The MMMs simulate ss positive and negative trends at Zeppelin (Jan.) and Esrange (May), respectively, but not ss positive trends at Utqiaġvik (April). Ss trends are simulated, but not observed, at Alert (January, December) and Tustervatn (March).

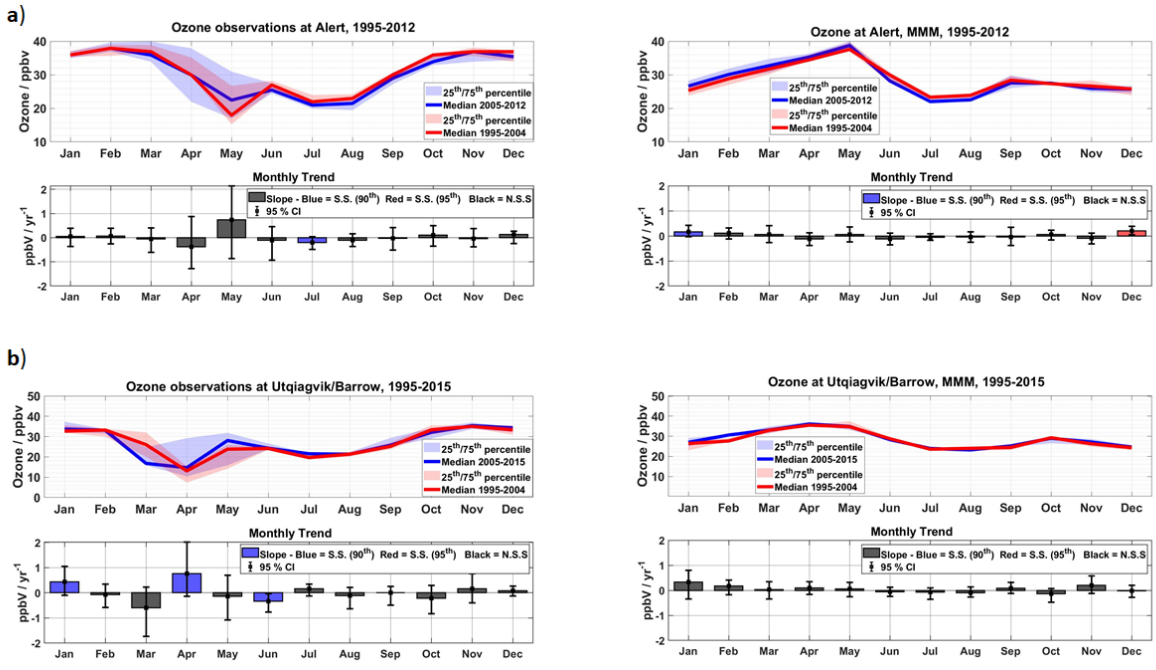

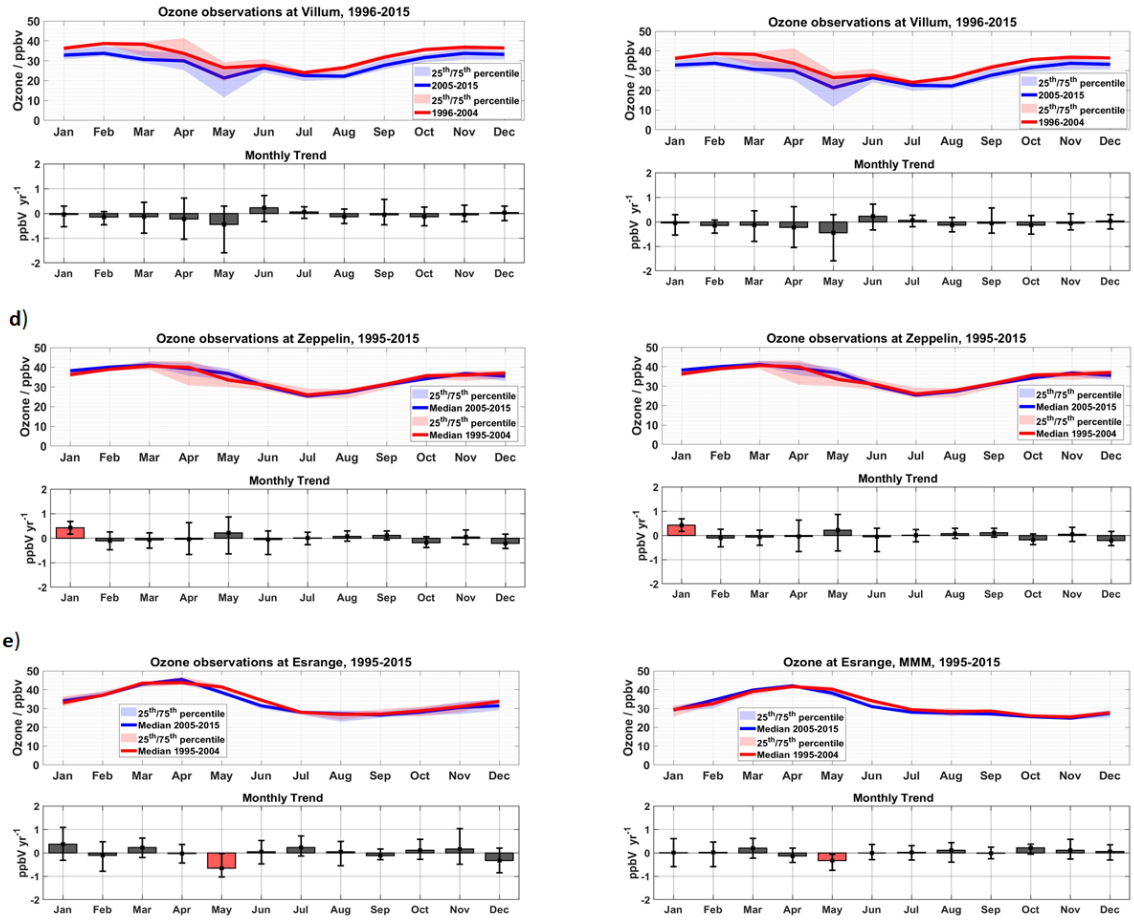


***Figure 3:*** *Comparison of observed (left) and MMM (right) surface $O_3$ trends and seasonal cycles at a) Alert, b) Utqiaġvik,* c) *Villum, d) Zeppelin, and e) Esrange. Upper panels: seasonal cycles for 1995-2004 (red lines) vs 2005-2015 (blue lines). Shaded areas show upper and lower quartiles of monthly values (observations only). Lower panels: monthly median trends in ppbv per year for 1995-2015, or shorter periods depending on data availability. Box coloring and error bars are the same as Fig. 2.*

# 4 Arctic ozone trends in the free troposphere

## 4.1 Observed vertical trends

This analysis focuses on $O_3$ changes in the lower and mid-troposphere. Figure 4 shows observed relative trends at six Arctic ozonesonde sites from 925-400 hPa for 1993-2019. Absolute trends above and below 400 hPa, and relative trends from 925-100 hPa, are also calculated (Figs. S7a,

S7b). Overall, while there are few ss trends, there seems to be a "dipole effect" with positive trends in winter and summer, and negative trends in spring and autumn. Positive ss winter (Jan/Dec) trends are found up to 400 hPa at most sites (except Resolute), and also at Scoresbysund in early spring. Positive wintertime trends are more evident in the earlier period in the upper troposphere (UT) and lower stratosphere (LS) (Fig. S8). Eureka, Resolute, and Sodankyla have periods with negative trends especially during spring and early summer in the lower troposphere. Resolute decreases extend up to 500 hPa in March-April. Relative ss trends vary from -1.5% to +0.5-1.0 % per year (Figs. 4, S7b) while stronger negative trends are diagnosed in later years (1999-2019) compared to 1993-2013 at all sites (Fig. S8).

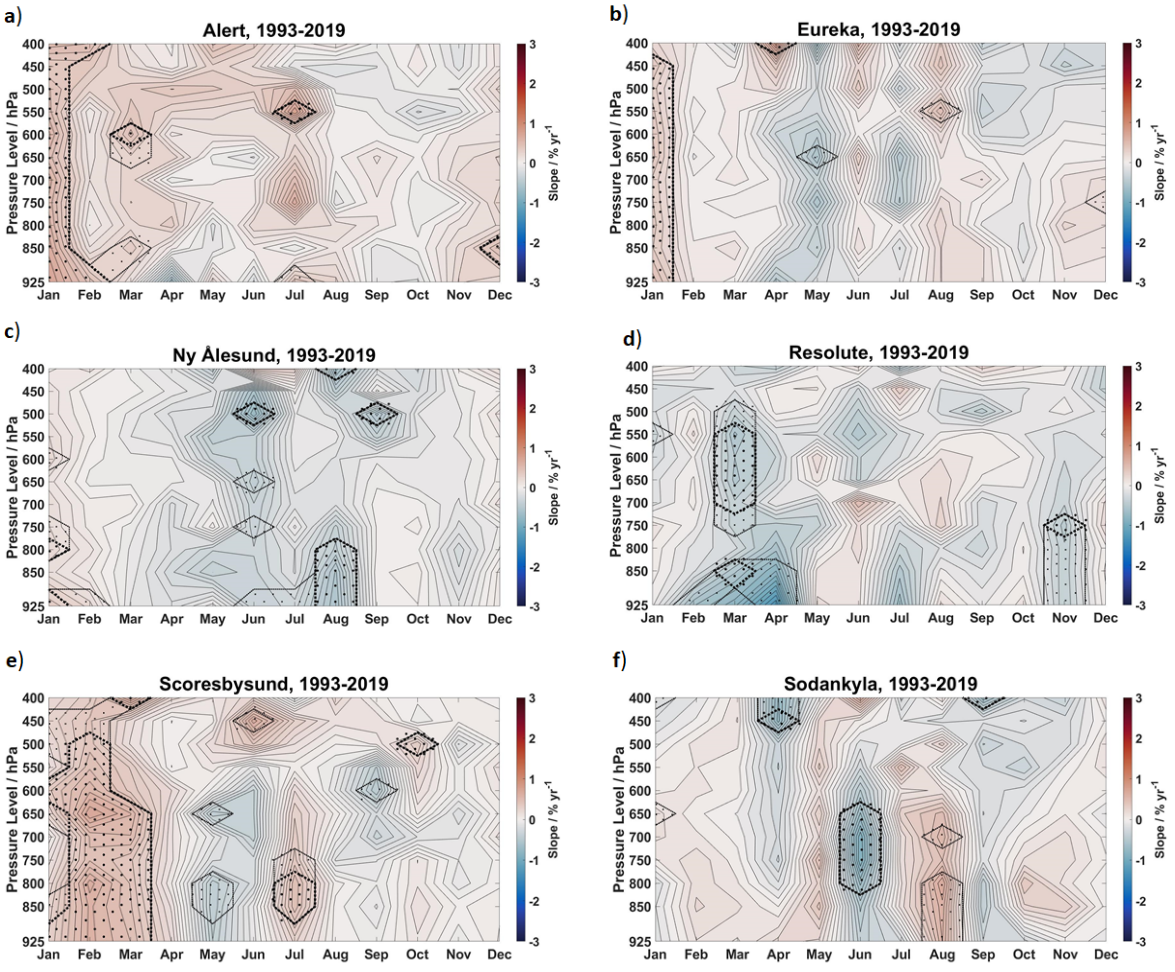


***Figure 4:*** *Vertical trends in observed monthly $O_3$ for 1993-2019, relative to monthly median concentrations, in % per year, from 925-400 hPa at a) Alert, b) Eureka, c) Ny Alesund, d) Resolute, e) Scoresbysund, and f) Sodankyla. Stippled lines/areas show statistical significance at the 90$^{th}$ % CL (smaller marker size) and 95$^{th}$ % CL (larger marker size).*

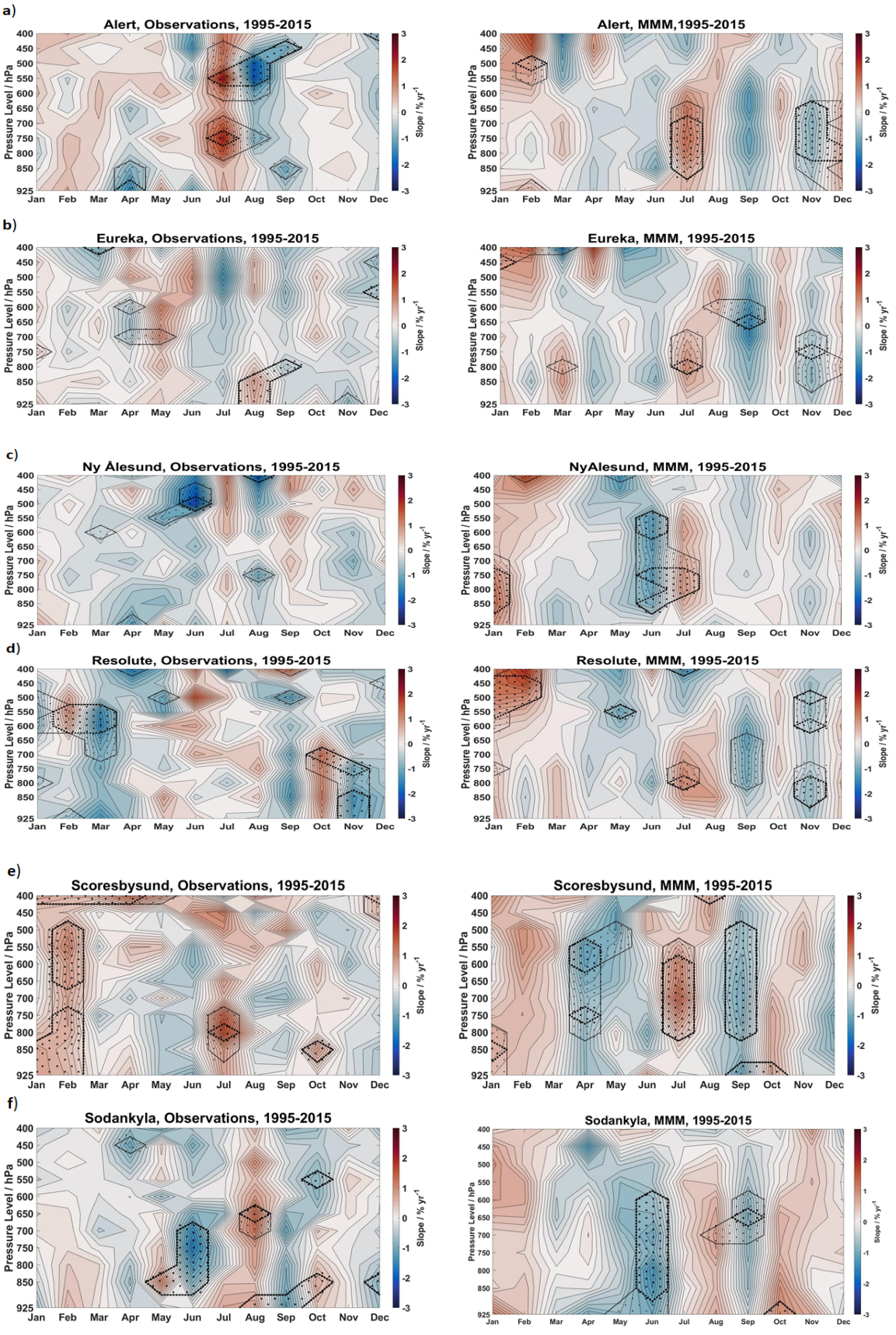
a)
Alert, Observations, 1995-2015
Alert, MMM,1995-2015
b)
Eureka, Observations, 1995-2015
Eureka, MMM, 1995-2015
c)
Ny Ålesund, Observations, 1995-2015
NyAlesund, MMM, 1995-2015
d)
Resolute, Observations, 1995-2015
Resolute, MMM, 1995-2015
e)
Scoresbysund, Observations, 1995-2015
Scoresbysund, MMM, 1995-2015
f)
Sodankyla, Observations, 1995-2015
Sodankyla, MMM, 1995-2015
Pressure Level / hPa
Slope / % yr-1
Jan Feb Mar Apr May Jun Jul Aug Sep Oct Nov Dec

***Figure 5:*** *Comparison of observed (left) and MMM (right) vertical trends in monthly $O_3$, relative to monthly medians, in % per year, from 925-400 hPa over 1995-2015 at a) Alert, b) Eureka, c) Ny Alesund, d) Resolute, e) Scoresbysund, and f) Sodankyla. Shading/symbols are as in Fig. 4.*

### 4.2 Comparison of observed and modeled vertical trends

Figure 5 shows observed ozonesonde and MMM trends for 1995-2015 up to 400 hPa (see Fig. S9 for results up to 100 hPa). Only results from 5 models are used, since EMEP MSC-W only provided surface $O_3$. The MMMs appear to capture the observed "dipole effect" seen in the observed trends. Models also capture observed increases in the winter but trends are overestimated at most sites, especially Ny Alesund and Sodankyla. Negative winter trends at Resolute are not simulated. This may be linked to positive modeled trends above 500 hPa at all sites (Fig. S9). Summertime positive ss MMM trends are larger than observed trends at some sites, e.g. Resolute and Ny Alesund.

## 5 Discussion and conclusions

Increasing annual surface $O_3$ trends at Arctic coastal sites, and at Zeppelin, are in qualitative agreement with Cooper et al. (2020), but in contrast to negative or non-significant surface trends at Canadian ozonesonde sites (Tarasick et al., 2016). A notable finding is that ss positive trends occur mainly in the winter months. While such increases were reported previously at Utqiaġvik (Gaudel et al. 2018; Christiansen et al., 2022) and Alert (Sharma et al., 2019), we confirm this tendency over the wider Arctic. Emission reductions of $NO_x$ in Europe and North America, and more recently over eastern Asia, have led to increasing wintertime $O_3$ at mid-latitudes due to less NO titration of $O_3$ (Jhun et al., 2015, Wang et al., 2022b, Bowman et al., 2022). This can explain observed increases in wintertime surface Arctic $O_3$, influenced primarily by transport of air masses from Europe (Hirdman et al., 2010). Evidence for declining $O_3$ precursor trends is supported by decreases in observed CO in the Arctic during autumn and winter (Fig. S10). At the same time, $CH_4$ continues to increase globally contributing to rising $O_3$ in the NH (Zeng et al., 2022) (see also Text S4 on Arctic $O_3$ precursor trends).

Another intriguing finding is springtime ss surface $O_3$ increases at Utqiaġvik (especially over 1999-2019, Fig S4), but no ss changes at Alert and Villum. Changes in $O_3$ concentrations at this

time of year may be driven by changes in ODE frequency linked to climate change or weather patterns (Oltmans et al, 2012). ODEs lead to zero or very low springtime $O_3$ due to bromine released from frost flowers or blowing snow (on sea-ice) (Simpson et al., 2007) or iodine compounds with a possible oceanic source (Benevant et al., 2022). Increases in springtime tropospheric bromine oxide have been observed from satellites, especially along the north coast of Greenland and central Arctic Ocean, correlating weakly with an increasing frequency in first year sea-ice (Bougoudis et al., 2020). Indeed, the frequency of low springtime $O_3$ concentrations has been increasing at Canadian high Arctic sites (see Fig. S11) but no ss springtime monthly trends are determined at Alert or Villum in our analysis. Springtime increases at Utqiaġvik could be due to stronger transport from mid-latitudes to this site during periods with a more northerly extension of the Pacific storm track, hampering conditions for ODEs (Koo et al., 2012). They could also be due to an increasing influence from local emissions, such as shipping or Alaskan petroleum extraction, when photochemistry becomes active in spring (Gunsch et al., 2017).

Decreases in springtime/early summer $O_3$ in northern Scandinavia, especially over the later 1999-2019 period, are consistent with negative trends reported at Tustervatn (Cooper et al., 2020), and sites in northern Sweden during summer (Andersson et al., 2017). These decreases are associated with lower maximum $O_3$ concentrations linked to reductions in European precursor emissions leading to less photochemical $O_3$ production (Cooper et al., 2020) although no ss trends in observed Arctic CO are found at this time of year (Fig. S10). Springtime ss negative trends at Summit may also be due to emission reductions over North America. Our results do not suggest a shift in the $O_3$ seasonal cycle toward higher concentrations in the spring (i.e. moving back toward pre-industrial $O_3$ seasonality) as reported at NH mid-latitudes (Bowman et al., 2022). Another explanation for decreasing springtime $O_3$ at the surface could be that reductions in snow cover (Mudryk et al., 2020) are leading to more $O_3$ dry deposition to Scandinavian forests.

The observed and modeled surface trend comparison covers 1995-2015, thereby missing the later time period when stronger observed $O_3$ trends are found, especially ss positive trends in winter. MMMs capture wintertime $O_3$ increases at Zeppelin, but overestimate at Alert and miss increase at Utqiaġvik. However, Whaley et al. (2023) noted that these models underestimate wintertime Arctic $O_3$ due to deficiencies modeling shallow boundary layers, $O_3$ deposition or $NO_x$ lifetimes.

Nevertheless, decreasing winter trends in surface CO are captured at Alert and Utqiaġvik (Fig. S10). Ss positive spring $O_3$ trend at Utqiaġvik is not evident in MMM trends over 1995-2015. However, the models do not capture springtime $O_3$ seasonality due to incorrect simulation of transport patterns (Oltmans et al., 2012) or missing surface halogen chemistry (Whaley et al., 2023). Negative ss springtime (May) trends are not always reproduced, possibly reflecting issues in the emission trends or modeled dry deposition.

FT $O_3$ trends are ss positive in winter at all Arctic sites, except Resolute, in common with several coastal Arctic surface sites. These results are in-line with increases reported at NH mid-latitudes (Cooper et al., 2020), and at Canadian ozonesonde sites (up to 400 hPa), except Resolute (Wang et al., 2022a). MMM trends are similar to observed trends over 1995-2015, including where they are ss. Patterns in observed trends are quite well captured, notably positive ss trends in winter and summer, although they tend to be overestimated. Observed negative trends in spring, extending from near the surface into the FT, are generally reproduced, and are likely to be due to decreasing $NO_x$ emissions leading to lower FT $O_3$ where photochemical production is $NO_x$-limited. Overestimation of winter trends contrasts to previous studies where models underestimated NH trends (Wang et al., 2022a; Christiansen et al., 2022). This may be due to differences in model transport or $O_3$ precursor emission trends, including $NO_x$ reductions (see also Text S4). AMAP models overestimate mid-latitude FT $O_3$ (Whaley et al., 2023), possibly suggesting a larger sensitivity to precursor emission changes.

Observed trends in the UT (LS) appear to have switched from positive to negative since 1993 in winter/spring, which may explain stronger positive FT trends in the earlier part of the record (1993-2013). More frequent positive phases of the Arctic Oscillation in recent years may be contributing with a weaker Brewer-Dobson circulation leading to less transport of stratospheric $O_3$ into the Arctic UT-LS, a higher tropopause height, and thus lower $O_3$ concentrations in this region (Zhang et al., 2017). However, Liu et al. (2020) did not detect any trend in the stratospheric $O_3$ flux into the Arctic UT. On the other hand, Wang et al. (2022a) attributed FT increases in NH mid-high latitude $O_3$ to increases in aircraft $NO_x$ emissions.

Overall, this study finds significant robust trends in Arctic tropospheric $O_3$. Observed trends are generally quite well captured by multi-model median results, although for example, they

overestimate wintertime free tropospheric increases, and miss Alaskan surface increases in spring. Further investigation into the causes of observed trends, and model performance, are needed taking into account uncertainties in the observations and models (Young et al., 2018; Fiore et al., 2022).

# Acknowledgements

We thank colleagues involved in AMAP (2021), notably K. von Salzen (Env. Canada), M. Flanner (U. Michigan). Technicians and logistical support staff are gratefully acknowledged for their work on data collection: D. Worthy (Alert), K. Sjöberg (Esrange), K. Saarnio (Pallas), B. Jensen, C. Christoffersen, K. Mortensen (Villum), and B. Thomas (Utqiaġvik/Barrow). None of the authors declare any real or perceived financial conflicts of interests. Multiple funders are acknowledged for support (see author metadata).

# Data Availability Statement:

Surface $O_3$ monitoring datasets are provided by EMEP (European Monitoring and Evaluation Program), and Global Atmosphere Watch (GAW) World Data Centre for Reactive Gases. EMEP and GAW $O_3$ data are available via the EBAS data portal (from end of 1989 to present). CO data at Utqiaġvik/Barrow and Zeppelin are also available via the EBAS data portal: http://ebas.nilu.no. Select the station name, and the component (CO, $O_3$) to access the data files. Canadian surface $O_3$ data can be downloaded from: https://data-donnees.ec.gc.ca/data/air/monitor/networks-and-studies/alert-nunavut-ground-level-ozone-study/. Canadian surface CO is available at: https://data-donnees.ec.gc.ca/data/air/monitor/national-air-pollution-surveillance-naps-program/?lang=en. Click on folders Data, Year, ContinuousData, then HourlyData. Surface $O_3$ records for Utqiaġvik/Barrow (BRW) and Summit (SUM) are provided by PE and IE via NOAA GML. Data is available at https://gml.noaa.gov/aftp/data/ozwv/SurfaceOzone/. Click on the directories for BRM or SUM to obtain the data. Surface $O_3$ measurements at Summit are made possible via the U.S. National Science Foundation Office of Polar Programs and their contract with Battelle Arctic Research Operations (contract #49100420C0001). Ny Ålesund, Scoresbysund and Sodankylä ozonesonde data are obtained as part of the Network for the Detection of Atmospheric

Composition Change (NDACC). Data is available via https://ndacc.larc.nasa.gov/index.php/stations. Click on the relevant site location to access the data files. Ozonesonde data for Alert, Resolute and Eureka have been reprocessed according to Tarasick et al. (2016), available at https://hegiftom.meteo.be/datasets/ozonesondes.

All model output files in NetCDF format from the simulations used in this study can be found here: https://open.canada.ca/data/en/dataset/c9a333ea-b81c-4df3-9880-ea7c3daeb76f. Model codes for GISS-E2.1 are available at: https://www.giss.nasa.gov/tools/modelE/.

Open-source codes for the Mann-Kendall test associated with Sen's slope are distributed under the BSD 3-Clause License in dedicated GitHub repositories hosted within the "mannkendall" organization (https://github.com/mannkendall), a Matlab (Collaud Coen and Vogt, 2020, https://doi.org/10.5281/zenodo.4134618, https://github.com/mannkendall/Matlab), Python (Vogt, 2020, https://doi.org/10.5281/zenodo.4134435, https://github.com/mannkendall/Python), and R (Bigi and Vogt, 2020, https://doi.org/10.5281/zenodo.4134632, https://github.com/mannkendall/R). Last access for all codes 27 January 2023.

# References

AMAP. (2015). AMAP Assessment 2015: Black carbon and ozone as Arctic climate forcers. *Arctic Monitoring and Assessment Programme (AMAP)*, 116, ISBN 978-82-7971-092-9. https://www.amap.no/documents/doc/amap-assessment-2015-black-carbon-and-ozone-as-arctic-climate-forcers/1299

AMAP (2021). AMAP Assessment 2021: Impacts of short-lived climate forcers on Arctic climate, air quality, and human health. Arctic Monitoring and Assessment Programme (AMAP), Tromsø, Norway, in press, 2023. Last access 24 January 2023. https://www.amap.no/documents/doc/amap-assessment-2021-impacts-of-short-lived-climate-forcers-on-arctic-climate-air-quality-and-human-health/3614

Andersson, C., Alpfjord, H., Robertson, L., Karlsson, P. E., & Engardt, M. (2017) Reanalysis of and attribution to near-surface ozone concentrations in Sweden during 1990–2013, *Atmospheric Chemistry and Physics, 17*, 13869–13890, https://doi.org/10.5194/acp-17-13869-2017.

Anenberg, S. C., Horowitz, L. W., Tong, D. Q., & West, J. J. (2010). An estimate of the global burden of anthropogenic ozone and fine particulate matter on premature human mortality using atmospheric modeling. *Environmental Health Perspectives*, *118*(9), 1189–1195. https://doi.org/10.1289/ehp.0901220

371 Arnold, S. R., Lombardozzi, D., Lamarque, J.-F., Richardson, T., Emmons, L. K., Tilmes, S., et al.
372 (2018). Simulated global climate response to tropospheric ozone-induced changes in plant
373 transpiration. *Geophysical Research Letters*, *45*(23), 13070–13079.
374 https://doi.org/10.1029/2018GL079938

375 Bahramvash Shams, S., Walden, V. P., Petropavlovskikh, I., Tarasick, D., Kivi, R., Oltmans, et al. (2019)
376 Variations in the vertical profile of ozone at four high-latitude Arctic sites from 2005 to 2017,
377 *Atmospheric Chemistry and Physics, 19*, 9733–9751, https://doi.org/10.5194/acp-19-9733-2019

378 Barrie, L., Bottenheim, J., Schnell, R. et al. (1988) Ozone destruction and photochemical reactions at
379 polar sunrise in the lower Arctic atmosphere. *Nature, 334***,** 138–141.
380 https://doi.org/10.1038/334138a0

381 Benavent, N., Mahajan, A. S., Li, Q., Cuevas, C. A., Schmale, J., Angot, H., et al. (2022). Substantial
382 contribution of iodine to Arctic ozone destruction. *Nature Geoscience*, 15(10), 770–773.
383 https://doi.org/10.1038/s41561-022-01018-w

384 Bougoudis, I., Blechschmidt, A.-M., Richter, A., Seo, S., Burrows, J. P., Theys, N., & Rinke, A. (2020).
385 Long-term time series of Arctic tropospheric BrO derived from UV–VIS satellite remote sensing and
386 its relation to first-year sea ice. *Atmospheric Chemistry and Physics*, 20(20), 11869–11892.
387 https://doi.org/10.5194/acp-20-11869-2020

388 Bowman, H., Turnock, S., Bauer, S. E., Tsigaridis, K., Deushi, M., Oshima, N., et al. (2022). Changes in
389 anthropogenic precursor emissions drive shifts in the ozone seasonal cycle throughout the northern
390 midlatitude troposphere. *Atmospheric Chemistry and Physics*, 22(5), 3507–3524.
391 https://doi.org/10.5194/acp-22-3507-2022

392 Christiansen, A., Mickley, L. J., Liu, J., Oman, L. D., & Hu, L. (2022). Multidecadal increases in global
393 tropospheric ozone derived from ozonesonde and surface site observations: can models reproduce
394 ozone trends? *Atmospheric Chemistry and Physics*, 22(22), 14751–14782.
395 https://doi.org/10.5194/acp-22-14751-2022

396 Christiansen, B., Jepsen, N., Kivi, R., Hansen, G., Larsen, N., and Korsholm, U. S. (2017) Trends and
397 annual cycles in soundings of Arctic tropospheric ozone, *Atmospheric Chemistry and Physics,* 17,
398 9347–9364. https://doi.org/10.5194/acp-17-9347-2017

399 Clifton, O. E., Fiore, A. M., Massman, W. J., Baublitz, C. B., Coyle, M., Emberson, L., et al. (2020). Dry
400 deposition of ozone over land: Processes, measurement, and modeling. *Reviews of Geophysics*,
401 *58*(1). https://doi.org/e2019RG000670

402 Collaud Coen, M., Andrews, E., Bigi, A., Martucci, G., Romanens, G., Vogt, F. P. A., and Vuilleumier,
403 L. (2020) Effects of the prewhitening method, the time granularity, and the time segmentation on the
404 Mann–Kendall trend detection and the associated Sen's slope, *Atmospheric Measurement*
405 *Techniques, 13*, 6945-6964. https://doi/org/10.5194/amt-13-6945-2020

406 Cooper, O. R., Schultz, M. G., Schröder, S., Chang, K.-L., Gaudel, A., Benítez, G. C., et al. (2020).
407 Multi-decadal surface ozone trends at globally distributed remote locations. *Elementa: Science of the*
408 *Anthropocene*, *8*, 23. https://doi.org/10.1525/elementa.420

409 Dibb, J. E. (2007). Vertical mixing above Summit, Greenland: Insights into seasonal and high frequency
410 variability from the radionuclide tracers 7Be and 210Pb. *Atmospheric Environment*, 41(24), 5020–
411 5030. https://doi.org/10.1016/j.atmosenv.2006.12.005

412 Fiore, A. M., Hancock, S. E., Lamarque, J.-F., Correa, G. P., Chang, K.-L., Ru, M., et al. (2022).
413 Understanding recent tropospheric ozone trends in the context of large internal variability: a new
414 perspective from chemistry-climate model ensembles. *Environmental Research: Climate*, 1(2),
415 025008. https://doi.org/10.1088/2752-5295/ac9cc2

416 Gaudel, A., Cooper, O. R., Ancellet, G., Barret, B., Boynard, A., Burrows, J. P., et al. (2018).
417 Tropospheric Ozone Assessment Report: Present-day distribution and trends of tropospheric ozone
418 relevant to climate and global atmospheric chemistry model evaluation. *Elementa: Science of the*
419 *Anthropocene*, *6*, 39. https://doi.org/10.1525/elementa.291

420 Griffiths, P. T., Murray, L. T., Zeng, G., Shin, Y. M., Abraham, N. L., Archibald, A. T., et al. (2021).
421 Tropospheric ozone in CMIP6 simulations. *Atmospheric Chemistry and Physics, 21(5),* 4187–4218.
422 https://doi.org/10.5194/acp-21-4187-2021

423 Gunsch, M. J., Kirpes, R. M., Kolesar, K. R., Barrett, T. E., China, S., Sheesley, R. J., et al. (2017).
424 Contributions of transported Prudhoe Bay oil field emissions to the aerosol population in Utqiaġvik,
425 Alaska. *Atmospheric Chemistry and Physics, 17(17)*, 10879–10892. https://doi.org/10.5194/acp-17-
426 10879-2017

427 Hirdman, D., Sodemann, H., Eckhardt, S., Burkhart, J. F., Jefferson, A., Mefford, T., et al. (2010). Source
428 identification of short-lived air pollutants in the Arctic using statistical analysis of measurement data
429 and particle dispersion model output. *Atmospheric Chemistry and Physics*, 10(2), 669–693.
430 https://doi.org/10.5194/acp-10-669-2010

431 Jhun, I., Coull, B. A., Zanobetti, A., & Koutrakis, P. (2015). The impact of nitrogen oxides concentration
432 decreases on ozone trends in the USA. *Air Quality, Atmosphere and Health*, 8(3), 283–292.
433 https://doi.org/10.1007/s11869-014-0279-2

434 Koo, J. H., Wang, Y., Kurosu, T. P., Chance, K., Rozanov, A., Richter, A., et al. (2012) Characteristics of
435 tropospheric ozone depletion events in the Arctic spring: analysis of the ARCTAS, ARCPAC, and
436 ARCIONS measurements and satellite BrO observations. *Atmospheric Chemistry and Physics*,
437 12(20), 9909–9922. https://doi.org/10.5194/acp-12-9909-2012

438 Law, K. S., Stohl, A., Quinn, P. K., Brock, C. A., Burkhart, J. F., Paris, J.-D., et al. (2014). Arctic air
439 pollution: New insights from POLARCAT-IPY. *Bulletin of the American Meteorological Society*,
440 95(12), 1873–1895. https://doi.org/10.1175/bams-d-13-00017.1

441 Liu, J., Rodriguez, J. M., Oman, L. D., Douglass, A. R., Olsen, M. A., & Hu, L. (2020). Stratospheric
442 impact on the Northern Hemisphere winter and spring ozone interannual variability in the
443 troposphere. *Atmospheric Chemistry and Physics*, *20*(11), 6417–6433. https://doi.org/10.5194/acp-
444 20-6417-2020

445 Mudryk, L., Santolaria-Otín, M., Krinner, G., Ménégoz, M., Derksen, C., Brutel-Vuilmet, C., et al.
446 (2020). Historical Northern Hemisphere snow cover trends and projected changes in the CMIP6
447 multi-model ensemble. *The Cryosphere*, 14(7), 2495–2514. https://doi.org/10.5194/tc-14-2495-2020

448 Oltmans, S. J., Johnson, B. J., & Harris, J. M. (2012) Springtime boundary layer ozone depletion at
449 Barrow, Alaska: Meteorological influence, year-to-year variation, and long-term change, *Journal of*
450 *Geophysical Research,* 117, D00R18, https://doi.org/10.1029/2011JD016889

451 Rap, A., Richards, N. A. D., Forster, P. M., Monks, S. A., Arnold, S. R., and Chipperfield, M. P. (2015).
452 Satellite constraint on the tropospheric ozone radiative effect. *Geophysical Research Letters*, *42*(12),
453 5074–5081. https://doi.org/10.1002/2015GL064037

454 Sand, M., Berntsen, T. K., von Salzen, K., Flanner, M. G., Langner, J., & Victor, D. G. (2016). Response
455 of Arctic temperature to changes in emissions of short-lived climate forcers. *Nature Climate*
456 *Change*, 6(3), 286–289. https://doi.org/10.1038/nclimate2880

457 Schmale, J., Arnold, S. R., Law, K. S., Thorp, T., Anenberg, S., Simpson, W. R., Mao, J., and Pratt, K. A.
458 (2018) Local Arctic air pollution: A neglected but serious problem, *Earth's Future*, 6, 1385-1412.
459 https://doi.org/10.1029/2018ef000952

460 Schmeisser, L., Backman, J., Ogren, J. A., Andrews, E., Asmi, E., Starkweather, S., et al. (2018).
461 Seasonality of aerosol optical properties in the Arctic. *Atmospheric Chemistry and Physics*, 18(16),
462 11599–11622. https://doi.org/10.5194/acp-18-11599-2018

463 Sen, P. K. (1968), Estimates of the regression coefficient based on Kendall's Tau, *Journal of the*
464 *American Statistical Association, 63*, 1379-1389. https://doi.org/10.1080/01621459.1968.10480934

465 Sharma, S., L. A. Barrie, E. Magnusson, G. Brattstrom, W. R. Leaitch, A. Steffen and S. Landsberger
466 (2019) A factor and trends analysis of multidecadal lower tropospheric observations of Arctic
467 Aerosol Composition, Black Carbon, Ozone, and Mercury at Alert, Canada. *Journal of Geophysical*
468 *Research-Atmospheres, 124*(24): 14133-14161. https://doi.org/10.1029/2019JD030844

469 Simpson, W. R., von Glasow, R., Riedel, K., Anderson, P., Ariya, P., Bottenheim, J., et al. (2007).
470 Halogens and their role in polar boundary-layer ozone depletion. *Atmospheric Chemistry and*
471 *Physics*, *7*(16), 4375–4418. https://doi.org/10.5194/acp-7-4375-2007

472 Tarasick, D. W., Davies, J., Smit, H. G. J., & Oltmans, S. J. (2016). A re-evaluated Canadian ozonesonde
473 record: measurements of the vertical distribution of ozone over Canada from 1966 to 2013.
474 *Atmospheric Measurement Techniques*, *9*(1), 195–214. https://doi.org/10.5194/amt-9-195-2016

475 Tarasick, D., Galbally, I.E., Cooper, O.R., Schultz, M.G., Ancellet, G., Leblanc, et al. (2019).
476 Tropospheric Ozone Assessment Report: Tropospheric ozone from 1877 to 2016, observed levels,

trends and uncertainties. *Elementa: Science of the Anthropocene, 7*: 39. https://doi.org/10.1525/elementa.376

Theil, H. (1950) A rank-invariant method of linear and polynomial regression analysis, *Nederl. Akad. Wetensch., Proc., 53*, 386--392, https://ir.cwi.nl/pub/18446

Turnock, S. T., Allen, R. J., Andrews, M., Bauer, S. E., Deushi, M., Emmons, L., et al. (2020). Historical and future changes in air pollutants from CMIP6 models. *Atmospheric Chemistry and Physics*, 20(23), 14547–14579. https://doi.org/10.5194/acp-20-14547-2020

von Salzen, K., Whaley, C. H., Anenberg, S. C., Van Dingenen, R., Klimont, Z., Flanner, M. G., et al. (2022). Clean air policies are key for successfully mitigating Arctic warming. *Communications Earth & Environment*, 3(1), 222. https://doi.org/10.1038/s43247-022-00555-x

Wang, H., X. Lu, D. J. Jacob, O. R. Cooper, K.-L. Chang, K. Li, et al. (2022a) Global tropospheric ozone trends, attributions, and radiative impacts in 1995-2017: an integrated analysis using aircraft (IAGOS) observations, ozonesonde, and multi-decadal chemical model simulations, *Atmospheric Chemistry and Physics*, *22,* 13753-13782. https://doi.org/10.5194/acp-22-13753-2022

Wang, T, L. Xue, Z. Feng, J. Dai, Y. Zhang, & Y. Tan (2022b) *Environmental Research Letters,* 17**,** 063003, Ground-level ozone pollution in China: a synthesis of recent findings on influencing factors and impacts. https://doi.org/10.1088/1748-9326/ac69fe

Whaley, C. H., Mahmood, R., von Salzen, K., Winter, B., Eckhardt, S., Arnold, et al. (2022), Model evaluation of short-lived climate forcers for the Arctic Monitoring and Assessment Programme: a multi-species, multi-model study, *Atmospheric Chemistry and Physics, 22*, 5775–5828. https://doi.org/10.5194/acp-22-5775-2022

Whaley, C. H., Law, K. S., Hjorth, J. L., Skov, H., Arnold, S. R., Langner, J., Pernov, et al. (2023), Arctic tropospheric ozone: assessment of current knowledge and model performance. *Atmospheric Chemistry and Physics*, 23, 637-661. https://doi.org/10.5194/acp-23-637-2023

Young, P.J., V. Naik, A. M. Fiore, A. Gaudel, J. Guo‖, M. Y. Lin, et al. (2018) Tropospheric Ozone Assessment Report: Assessment of global-scale model performance for global and regional ozone distributions, variability, and trends. *Elementa: Science of the Anthropocene*, 6: 10. https://doi.org/10.1525/elementa.265

Zeng, G., Morgenstern, O., Williams, J. H. T., O'Connor, F. M., Griffiths, P. T., Keeble, J., et al. (2022). Attribution of stratospheric and tropospheric ozone changes between 1850 and 2014 in CMIP6 models. *Journal of Geophysical Research: Atmospheres*, 127. https://doi.org/10.1029/2022JD036452

Zhang, J., F. Xie, W. Tian, Y. Han, K. Zhang, Y. Qi et al. (2017) Influence of the Arctic Oscillation on the vertical distribution of wintertime ozone in the stratosphere and upper troposphere over the Northern Hemisphere, *Journal of Climate*, 30(8). https://doi.org/10.1175/JCLI-D-16-0651.1

*Geophysical Research Letters*

Supporting Information for

# Arctic Tropospheric Ozone Trends

K. S. Law[1], J. Liengaard Hjorth[2], J. B. Pernov[2,3], C. H. Whaley[4], H. Skov[2], M. Collaud Coen[5], J. Langner[6], S. R. Arnold[7], D. Tarasick[8], J. Christensen[2], M. Deushi[9], P. Effertz[10,14], G. Faluvegi[11,12], M. Gauss[13], U. Im[2], N. Oshima[9], I. Petropavlovskikh[10,14], D. Plummer[4], K. Tsigaridis[11,12], S. Tsyro[13], S. Solberg[15] and S.T. Turnock[16,7]

[1]Sorbonne Université, LATMOS/IPSL, UVSQ, CNRS, Paris, France
[2]Department of Environmental Science, Interdisciplinary Centre for Climate Change, Aarhus University, Frederiksborgvej 4000, Roskilde, Denmark
[3]Extreme Environments Research Laboratory, École Polytechnique fédérale de Lausanne, 1951 Sion, Switzerland
[4]Canadian Centre for Climate modeling and analysis, Environment and Climate Change Canada, Victoria, BC, Canada
[5]Federal Office of Meteorology and Climatology, MeteoSwiss, Payerne, Switzerland
[6]Swedish Meteorological and Hydrological Institute, Norrköping, Sweden
[7]Institute of Climate and Atmospheric Science, School of Earth and Environment, University of Leeds, Leeds, United Kingdom
[8]Air Quality Research Division, Environment and Climate Change Canada, Toronto, ON, Canada
[9]Meteorological Research Institute, Japan Meteorological Agency, Tsukuba, Japan
[10]Cooperative Institute for Research in Environmental Sciences (CIRES), University of Colorado, Boulder, CO, USA.
[11]NASA Goddard Institute for Space Studies, New York, NY, USA
[12]Center for Climate Systems Research, Columbia University; New York, USA
[13]Norwegian Meteorological Institute, Oslo, Norway
[14]National Oceanic and Atmospheric Administration (NOAA) ESRL Global Monitoring Laboratory, Boulder, CO, USA.
[15]Norwegian Institute for Air Research (NILU), Kjeller, Norway.
[16]Met Office Hadley Centre, Exeter, UK

**Contents of this file**



## Introduction

The supporting information gives details about surface and ozonesonde data coverage (Text S1, Figs. S1 and S2), the trend analysis method (Text S2), and the models (Text S3) used in this study, and discusses trends of tropospheric ozone ($O_3$) precursors in the Arctic (Text S4). Additional figures show $O_3$ trends at Arctic locations not shown in the main text, and trends over different time periods for both the observations and models (Figs. S3-S9). Trends in surface carbon monoxide (CO) (Fig. S10), and in low springtime $O_3$ concentrations at Canadian Arctic

sites (Fig. S11) are also shown. Tables S1 and S2 provide additional details about the models and surface annual $O_3$ trends, respectively. See Fig. 1 in main text for measurement site locations.

**Text S1. Data coverage**

To ensure proper statistical representation of the data coverage thresholds at least 50% of available data is required for the calculation of monthly and annual trends. Data coverage for the surface sites is shown in Fig. S1. It is also verified that at least one complete year of data is available at the beginning and end of the time series, since incomplete years at the beginning and end of a time series can have a larger influence on trend analysis results (Collaud Coen et al., 2020). Esrange has full data coverage, with less than five months having coverage lower than 50%. Pallas, Summit, Tustervatn and Zeppelin have one to three periods of 1-2 years without data that do not preclude long-term trend analysis, although it should be noted that the Summit record only started in June 2000. Alert and Villum have a high monthly data coverage but suffer from missing data over a 4-5 year period in the middle of the time series. For Alert, there are two missing periods throughout the time series. For Villum there is only one missing period although the period 1996-2002 suffers from poor data coverage. Therefore, trends at Villum and Alert can be considered as valid but should be interpreted with caution (Collaud Coen et al., 2020).

Ozonesondes were launched at least once per week at the six Arctic stations used in this analysis. There are periods with up to three soundings a week, mostly in winter and spring (Fig. S2). Periods without measurements do not exceed 1 month except at Eureka, where there are five periods with missing data of three to eight months mostly in spring (2000, 2003, 2005, 2006, and 2016) and a 3-month period missing in 2006 at Sodankyla. The mean yearly number of soundings varies between 38 (Resolute) and 90 (Ny Ålesund). At Alert and Sodankyla a lower number of soundings were performed in 2016-2020. A visual inspection of the $O_3$ time series at the 20 pressure levels used in this analysis does not show evidence for any rupture apart from at the 4 lowest levels before 1995 at Eureka, potentially resulting in lower $O_3$ concentrations.

**Text S2. Trend analysis methodology**

Long-term trend determination needs to be applied to homogeneous time series in order to analyze real variations or changes in the observations as opposed to artifacts. For the surface $O_3$ concentrations, while data is taken from quality-controlled repositories, this does not take into account technical changes such as modification or changes in instrumentation, station position, changes to calibration procedures or instrumental drifts. Visual inspection allowed detection of potential ruptures in the time series.

Trends in surface $O_3$ concentrations at different sites are determined using the non-parametric Mann-Kendall test and Sen's slope methodology (Theil, 1950; Sen, 1968), and calculated using daily medians of the $O_3$ volume mixing ratios using hourly observations. These tests require the data to be serially independent and homogeneously distributed. However, the $O_3$ measurements are significantly lag-1 auto-correlated and exhibit high amounts of seasonality. Therefore, the data is prewhitened to remove the lag-1 autocorrelation. The seasonal Mann-Kendall test is applied to address the seasonality present in the data (Hirsch et al., 1982) using the Matlab version (Collaud Coen and Vogt, 2021) of the 3PW algorithm from Collaud Coen et al. (2020).

The 3PW method uses two prewhitening methods prior to testing for statistical significance. The first method from Kulkarni and von Storch (1995) simply removes the lag-1 autocorrelation (referred to as PW). This method has a low rate of false positives but lowers the power of the Mann-Kendall test. The second prewhitening method from Yue and Wang (2002), detrends the data before prewhitening (referred to as TFPW-Y). This method returns the power of the Mann-Kendall test although it increases the rate of false positives. Trends must be statistically significant using both methods to be considered significant in the 3PW algorithm. If a significant trend is present, then the slope is calculated using the variance corrected trend free prewhitening (VCTFPW) method from Wang et al. (2015), which gives an unbiased estimate of the Theil Sen slope. This method maximizes the advantages of these prewhitening methods and minimizes their disadvantages. We use the seasonal Mann-Kendall test on a monthly temporal segmentation (i.e., a trend analysis is performed on each value in a respective month over the period analyzed). For the $O_3$ soundings weekly resolution is applied since regular daily measurements are not available. Relative monthly trends (% per year) for the 20 pressure levels of the ozonesonde data are calculated as absolute monthly trends divided by monthly median concentrations x 100 %. Statistically significant (ss) trends are determined at the $90^{th}$ and $95^{th}$ % confidence levels (CLs). The Theil-Sen estimator is the median of all possible pairwise slopes. Upper CL and lower CL, on the $95^{th}$ % CL, contain the middle 95% of the pairwise slopes, which are normally distributed (Gilbert, 1987). To test the robustness of the results, trends are also compared for different periods of available records (1993-2019, 1993-2013, 1999-2019), and comparison with the model results (1995-2015). Monthly medians are used to compare model results with the observations since higher temporal resolution results are not available from the models. In all cases, model results are averaged to produce multi-model median (MMM) results.

For trends in the yearly median, a simple Mann-Kendall test and Theil Sen Slope without prewhitening are employed, using the MAKESENS application (Salmi et al., 2002), since there is no seasonality present, and the data are not autocorrelated. The minimum requirement for including observation series in this evaluation is data available from 1996 to 2018 in order to have comparable trends. Nearly all of the stations have years with less than 50% data coverage which are not included in the calculations of the annual trends. Relative trends are given as percentages of median concentrations.

**Text S3. Models**

Four global chemistry-climate (CMAM, GISS-E2.1, MRI-ESM2, UKESM1) and two chemistry-transport (DEHM, EMEP MSC-W) models were run using the same (ECLIPSEv6b) anthropogenic emissions for 1990 (1995 for GISS model) to 2015 as part of the Arctic Monitoring and Assessment Programme (AMAP) assessment (AMAP, 2021). They were run with different biogenic emissions and meteorology and nudged using different reanalysis products (see Table S1). The models also vary in their representation of the stratosphere with only a subset of having a fully simulated stratosphere. CMAM, MRI-ESM2, GISS-E2.1, and UKESM1 contain relatively complete stratospheric $O_3$ chemistry (involving nitrogen oxides ($NO_x$), chlorine and bromine chemistry), while the other models have no stratospheric chemistry (DEHM, EMEP MSC-W). Model results from 1995-2015 are used in this study.

Present-day model simulations for 2014-2015, including the models contributing to this study, were evaluated first against a limited set of tropospheric Arctic $O_3$ observations (Whaley et al., 2022), and also in more detail, including tropospheric Arctic $O_3$ seasonal cycles, in our companion paper Whaley et al. (2023). These evaluations show large variability in model performance. The MMMs capture surface Arctic $O_3$ observations quite well, except for low concentrations observed during high Arctic polar spring (Whaley et al., 2023). Most atmospheric models, including all of the models in this study, do not yet contain Arctic tropospheric halogen chemistry, and thus cannot simulate the surface-level bromine and iodine-driven $O_3$ depletion events that occur during spring at some Arctic locations (Whaley et al., 2023). Model performance in the free troposphere is better (within +/- 10%) compared to satellite, aircraft and ozonesonde data, but upper tropospheric $O_3$ is overestimated (Whaley et al., 2022, 2023).

**Text S4. Trends in tropospheric Arctic $O_3$ precursors**

To understand Arctic tropospheric $O_3$ trends, it is important to understand trends in $O_3$ precursors as well as other factors such as changing transport patterns. $O_3$ precursors include methane ($CH_4$), CO, $NO_x$ and non-methane volatile organic compounds (NMVOCs). While, as pointed out in the main text, precursor trends over Northern Hemisphere (NH) mid-latitude emission regions are likely contributing to changes in Arctic tropospheric $O_3$, it is also useful to examine precursor trends in the Arctic, when long-term measurements are available, and to evaluate MMM trends. The contribution of different sources, including precursor emissions, and sinks of Arctic $O_3$ is discussed in Whaley et al. (2023) and references therein.

Arctic $CH_4$ at the surface rose from 1.75 ppmv in 1984 to 1.95 ppmv in 2020 (AMAP, 2021). The increasing trend was interrupted by a plateau between 2000 and 2005 that accelerated after 2015 based on data from Pallas, Zeppelin and Utqiaġvik (formerly known as Barrow). AMAP (2021) derived an ss ($95^{th}$ % CL) observed annual trend of +2.29+/-0.55 ppbv per year, whereas modeled $CH_4$, which was prescribed, had an annual trend of +2.79 ppbv per year, ss only at $90^{th}$ % CL. Thus, modeled and measured trends are reasonably comparable. Around 40% of Arctic $O_3$ response to precursor emission changes may be due to increasing $CH_4$ (AMAP, 2015).

Mackie et al. (2016) showed that CO decreased from 1989-2012 at Utqiaġvik with the largest ss decreases in winter and spring attributed to decreasing anthropogenic CO emissions in Europe and North America. Figure S10 compares seasonal CO trends from observations and MMM results at the few sites with long time series (Alert, Utqiaġvik and Zeppelin). These trend calculations are based on monthly averages, applying the 3PW algorithm, as discussed in 2.3 and S2, for periods with available data. MMM results are in general agreement with the observations showing ss negative trends in winter and autumn. However, it can be noted that the models underestimate surface NH CO in winter (Whaley et al, 2023). This discrepancy is larger earlier in the time series, while the models agree better with observed CO later in the time series (not shown).

There are no reported trends in $NO_x$ or NMVOCs in the Arctic due to a lack of long-term measurements (AMAP, 2021). In general, observed NMVOC concentrations are low at Arctic sites monitoring background air masses, and away from local sources (Pernov et al. 2021). Thus,

local NMVOC photo-oxidation only has limited effect on Arctic tropospheric $O_3$ as discussed by Helmig et al. (2014) and Gautrois et al. (2003). However, long-range transport of air masses, influenced by mid-latitude anthropogenic and natural NMVOC emissions, can influence Arctic tropospheric $O_3$ (Whaley et al., 2023). $NO_x$ concentrations are also generally low in the background Arctic troposphere (Whaley et al., 2023), but can be elevated near local sources, for example due to shipping emissions (e.g. Marelle et al., 2016). Also, long-range transport of $NO_x$ reservoir species such as peroxy-acetyl nitrate (PAN) or nitric acid can decompose in the warmer spring and summer months producing $NO_x$ (Law et al. (2014) and refs therein). Walker et al. (2012) estimated that more than 50% of $O_3$ in the Arctic during summer is formed from local PAN decomposition. Whaley et al (2023) showed that MMMs underestimate CO and $NO_x$ throughout the troposphere, but overestimates PAN compared to observed aircraft profiles in the Arctic. Despite these differences, models match observed $O_3$ profiles in the troposphere, but significantly overestimates $O_3$ near the tropopause, as noted earlier.

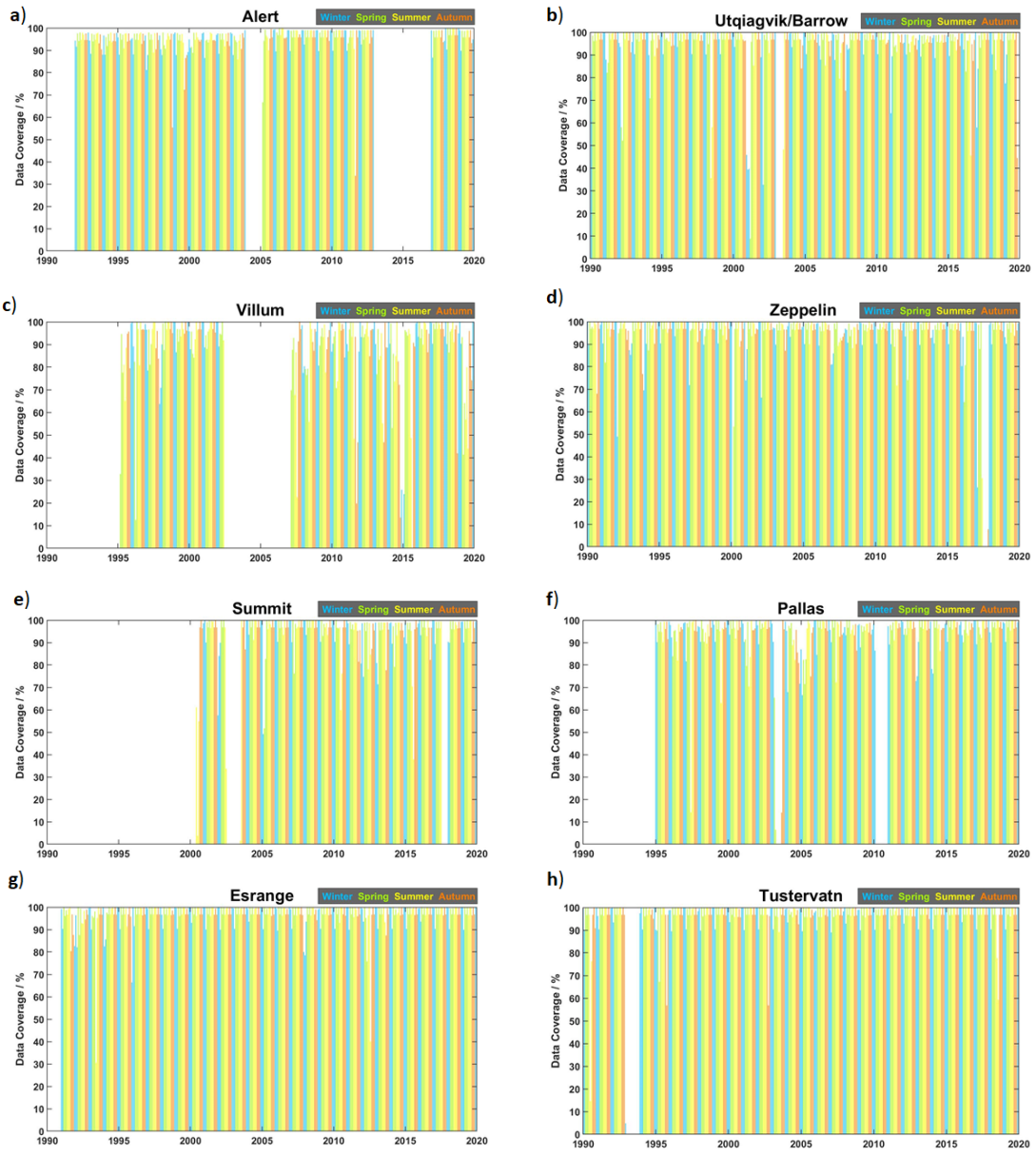


180

181

182 **Figure S1.** *Data coverage for surface $O_3$ measurements at a) Alert, b) Utqiaġvik, c) Villum, d)*
183 *Zeppelin, e) Summit, f) Pallas, g) Esrange, and h) Tustervatn. Coverage is given as a percentage*
184 *of hours with measurements compared to the total number of hours for each month. Monthly*
185 *coverage is color-coded by the meteorological seasons. See Figure 1 for station locations.*

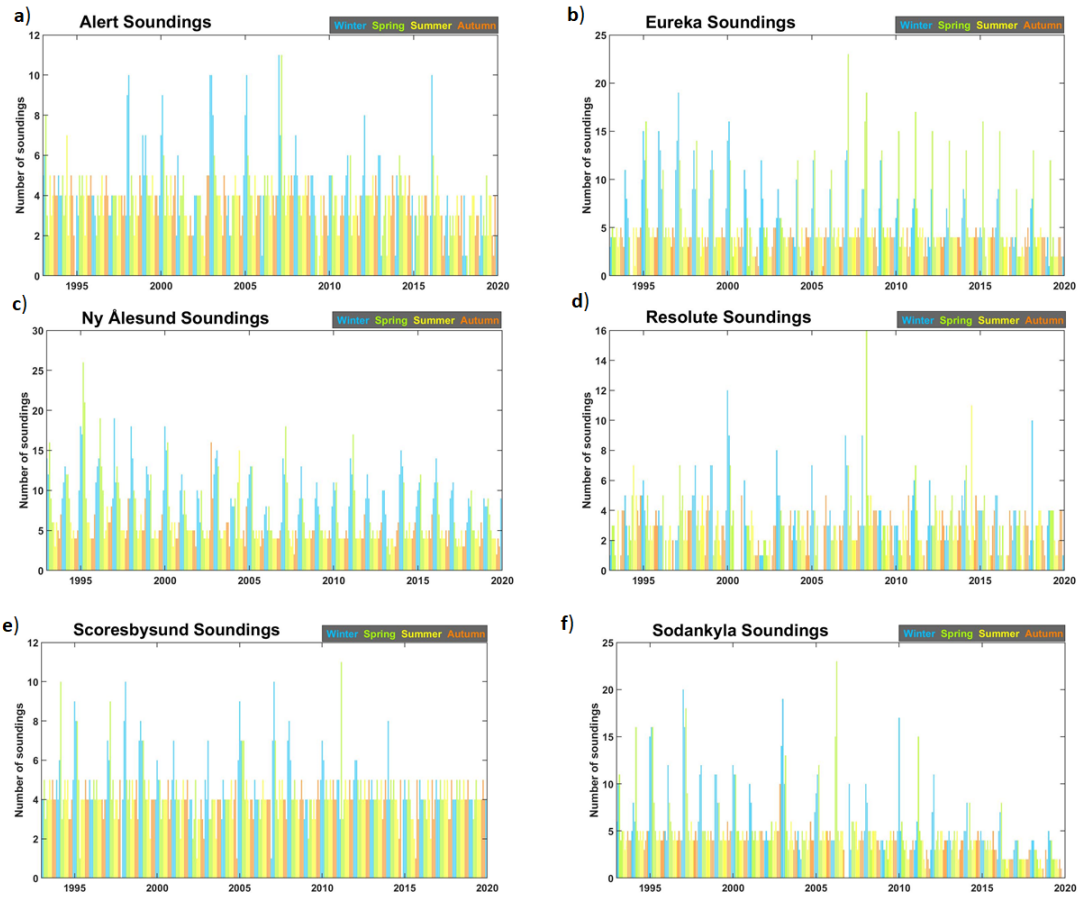


**Figure S2.** *Ozonesonde data coverage at a) Alert, b) Eureka, c) Ny Alesund, d) Resolute, e) Scoresbysund, and f) Sodankyla. The number of $O_3$ soundings in each month is shown color-coded by the meteorological seasons. See Figure 1 for station locations.*

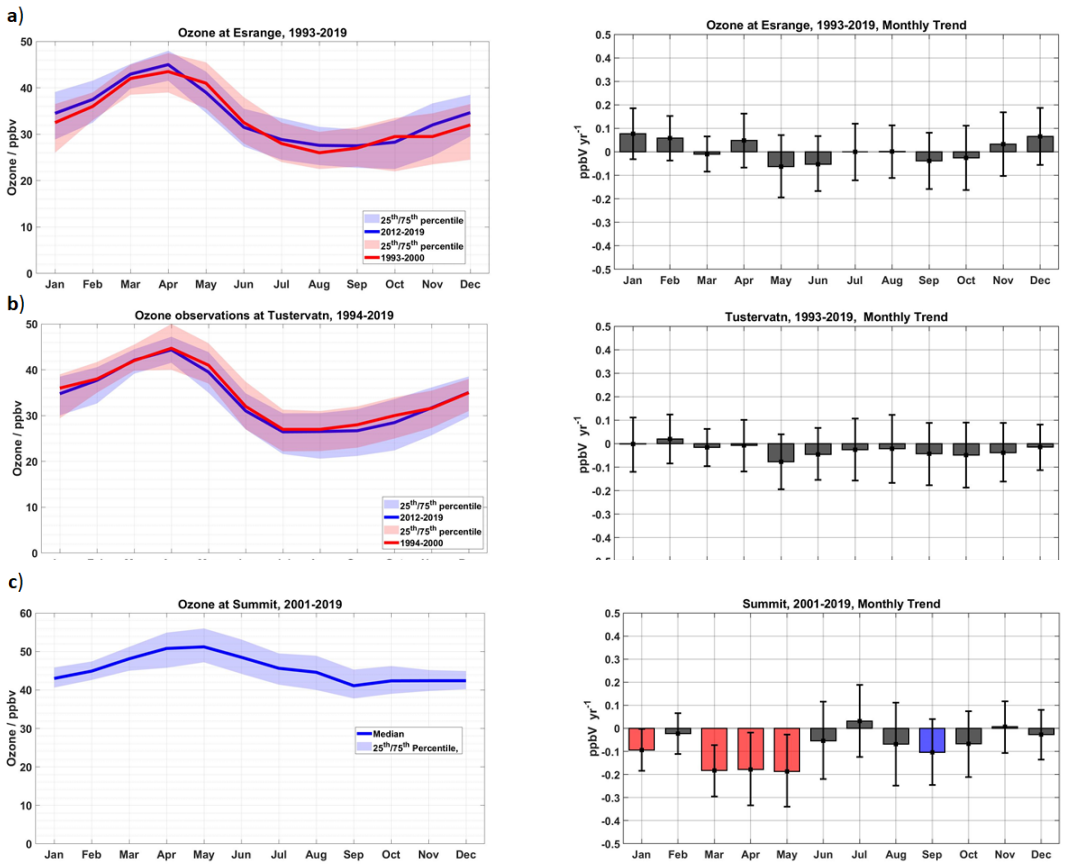


191

192

193 **Figure S3.** *Observed surface $O_3$ trends and seasonal cycles. Left panels: seasonal cycles of*
194 *monthly median $O_3$ (ppbv) at a) Esrange, and b) Tustervatn for 1993-2000 (blue lines) vs 2012-*
195 *2019 (red lines), and c) Summit for 2001-2019 only. Shaded areas show upper and lower*
196 *quartiles of hourly values. Right panels: monthly trends over 1993-2019, or for shorter periods*
197 *depending on data availability. Boxes represent the slope of the trend in ppbv per year with red*
198 *boxes significant at 95$^{th}$% CL, blue boxes at 90$^{th}$% CL, and black boxes not statistically*
199 *significant. Error bars show 95$^{th}$% CLs.*

200

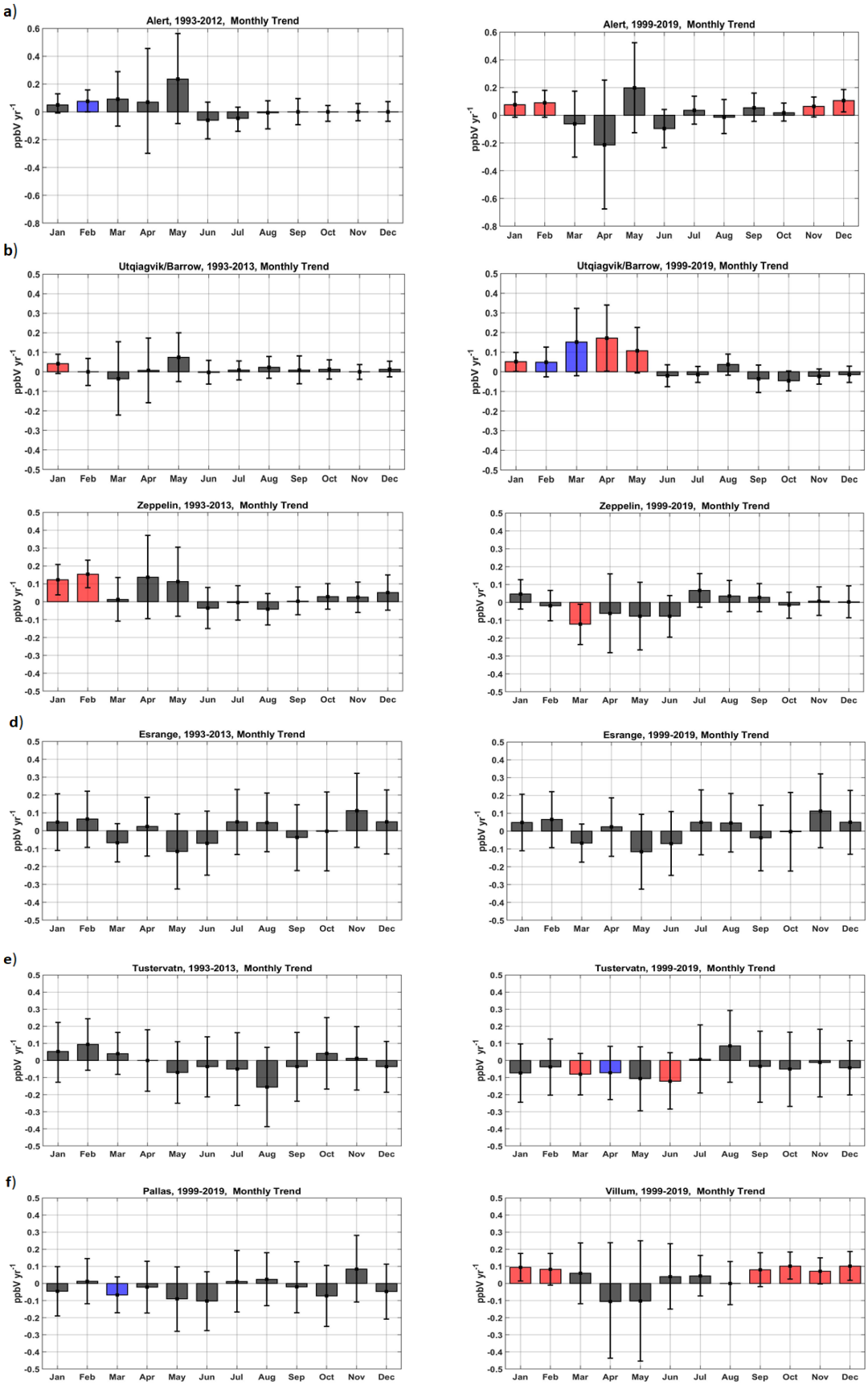
a)
Alert, 1993-2012, Monthly Trend
Alert, 1999-2019, Monthly Trend
b)
Utqiagvik/Barrow, 1993-2013, Monthly Trend
Utqiagvik/Barrow, 1999-2019, Monthly Trend
Zeppelin, 1993-2013, Monthly Trend
Zeppelin, 1999-2019, Monthly Trend
d)
Esrange, 1993-2013, Monthly Trend
Esrange, 1999-2019, Monthly Trend
e)
Tustervatn, 1993-2013, Monthly Trend
Tustervatn, 1999-2019, Monthly Trend
f)
Pallas, 1999-2019, Monthly Trend
Villum, 1999-2019, Monthly Trend
ppbV yr-1
Jan Feb Mar Apr May Jun Jul Aug Sep Oct Nov Dec

201

202

203

**Figure S4.** *Comparison of observed surface $O_3$ monthly median trends in ppbv per year for different time periods at a) Alert, b) Utqiaġvik, c) Zeppelin, d) Esrange, e) Tustervatn for 1993-2012 and 1999-2019, depending on data availability, and f) Pallas (left) and Villum (right) for 1999-2019, when good data coverage is available. Box coloring and error bars are the same as Fig. S3 (right panels).*

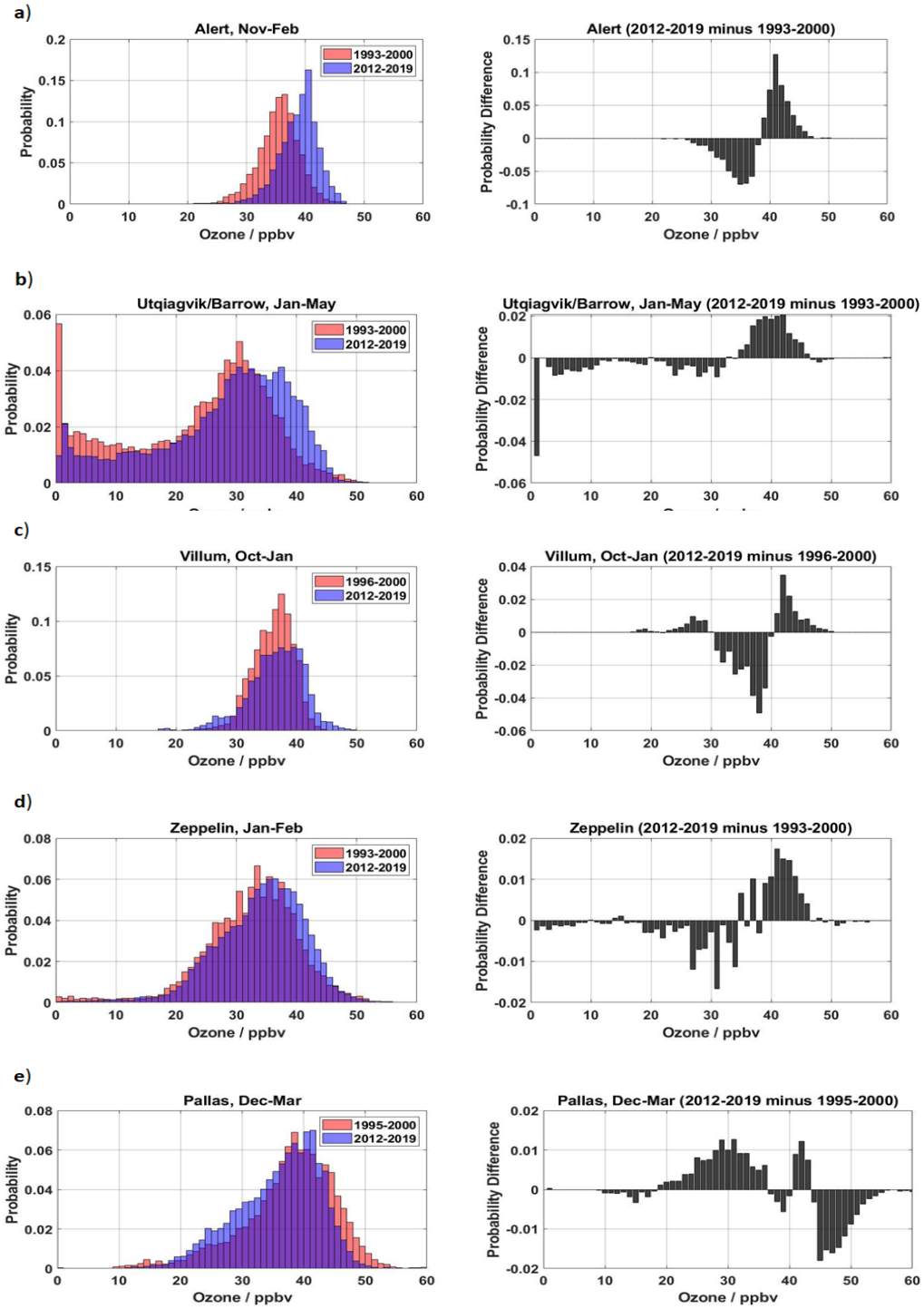


**Figure S5.** *Changes in probability distributions of surface $O_3$ concentrations in ppbv between earlier (1993-2000) and later (2012-2019) periods for selected months with statistically significant trends (see Figs. 2 and S3) at a) Alert, b) Utqiaġvik, c) Villum, d) Zeppelin, and e) Pallas. Periods shown vary depending on data availability.*

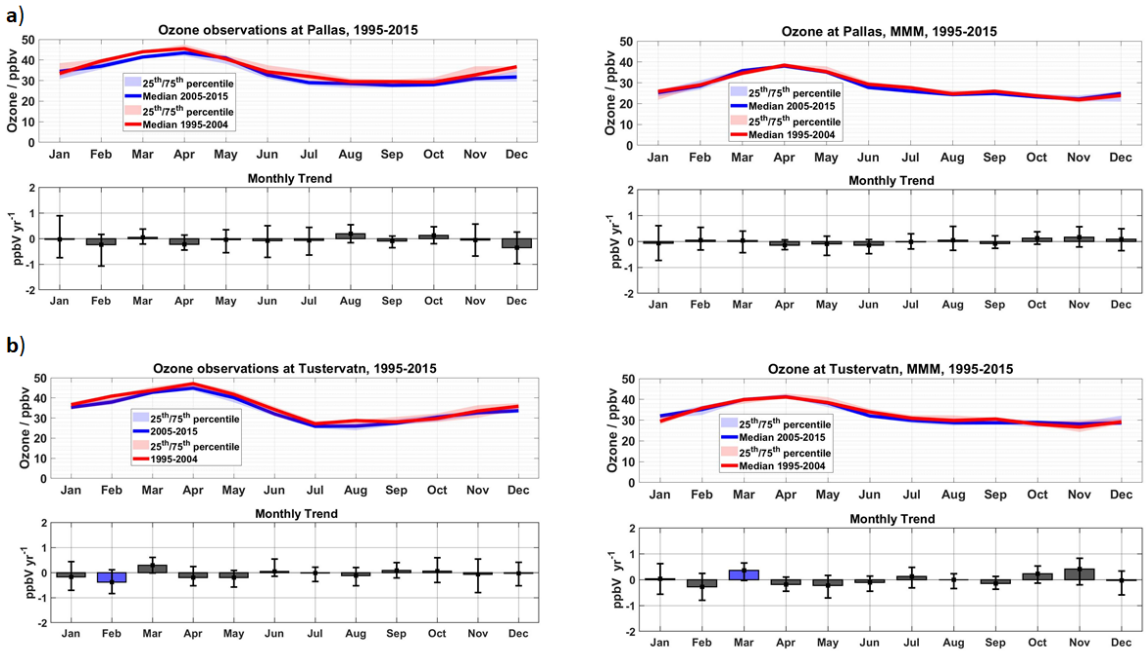


217

218 **Figure S6.** *Comparison of observed (left) and MMM (right) surface $O_3$ trends and seasonal*
219 *cycles at a) Pallas and b) Tustervatn. Upper panels: seasonal cycles for 1995-2004 (red lines) vs*
220 *2005-2015 (blue lines). Shaded areas show upper and lower quartiles of hourly values*
221 *(observations only). Lower panels: monthly median trends in ppbv per year for 1995-2015. Box*
222 *coloring and error bars are the same as Fig. S3. Shorter periods are shown depending on data*
223 *availability.*

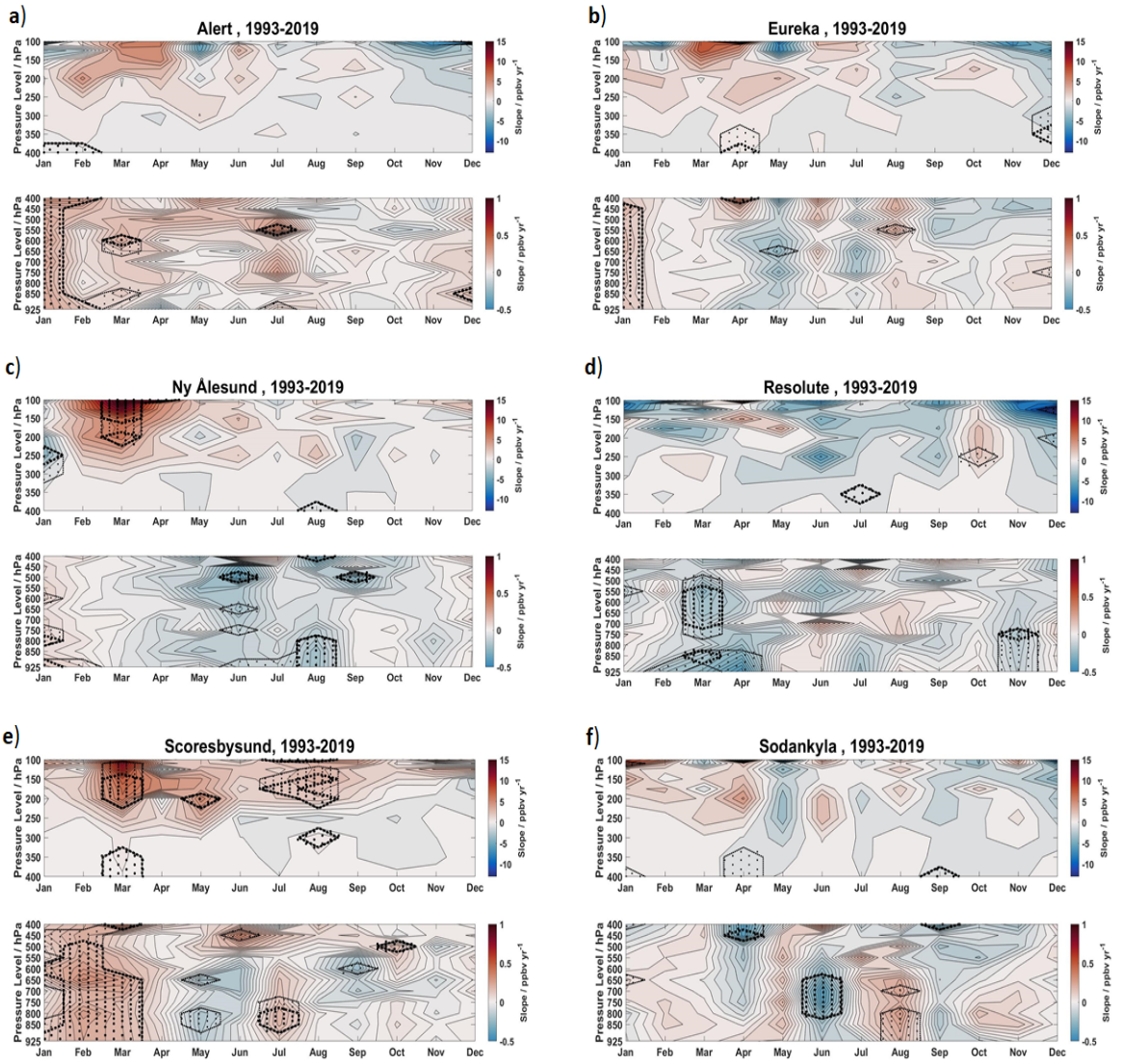


224

225

226 **Figure S7a.** *Absolute vertical trends in observed monthly $O_3$ for 1993-2019 in ppbv per year at a)*
227 *Alert, b) Eureka, c) Ny Alesund, d) Resolute, e) Scoresbysund and f) Sodankyla. Upper panels:*
228 *upper troposphere and lower stratosphere (400-100 hPa). Lower panels: mid- and lower*
229 *troposphere (925-400 hPa). Note the different color scales. Stippled lines/areas show statistical*
230 *significance at the 90$^{th}$ % CL (smaller marker size) and 95$^{th}$ % CL (larger marker size).*

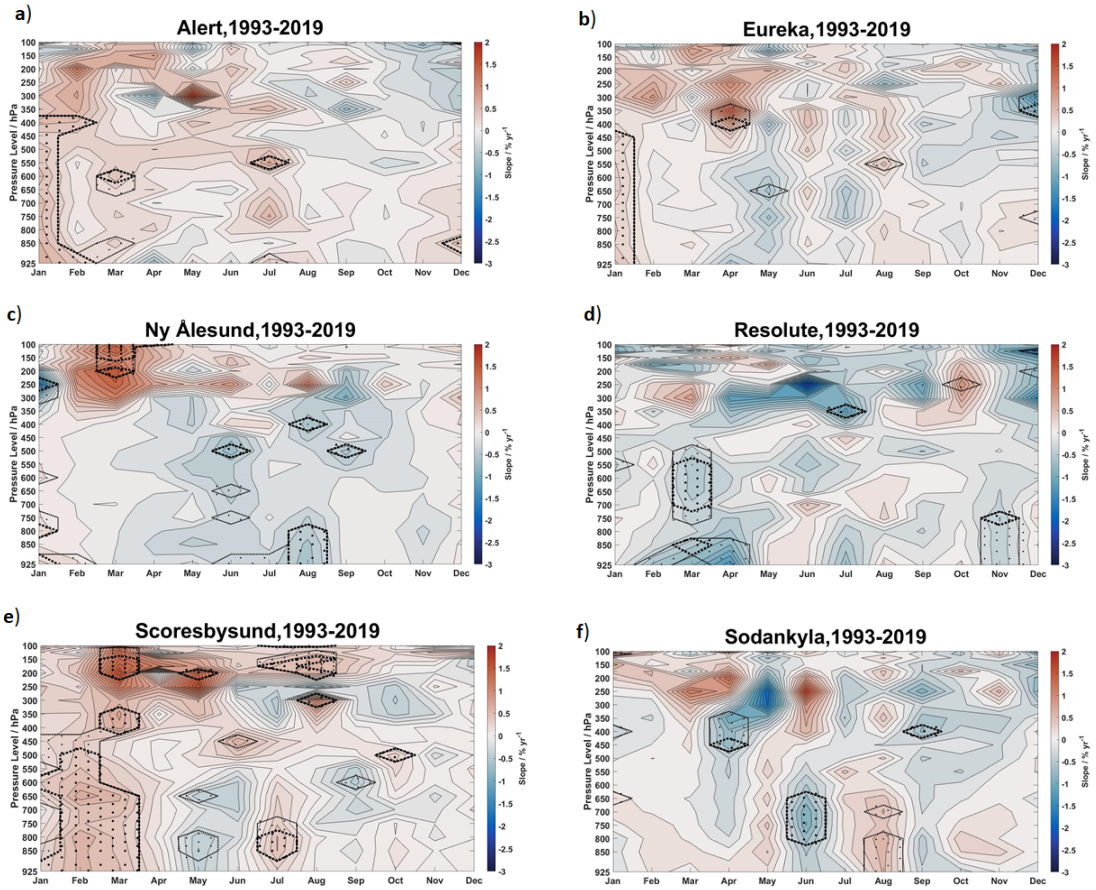


231

232

233

234 **Figure S7b:** *Same as Figure S7a, but vertical trends from 925-100 hPa in observed monthly $O_3$*

235 *for 1993-2019, relative to monthly median concentrations, in % per year. Shading and symbols*

236 *are the same as Fig S7a.*

237

a)

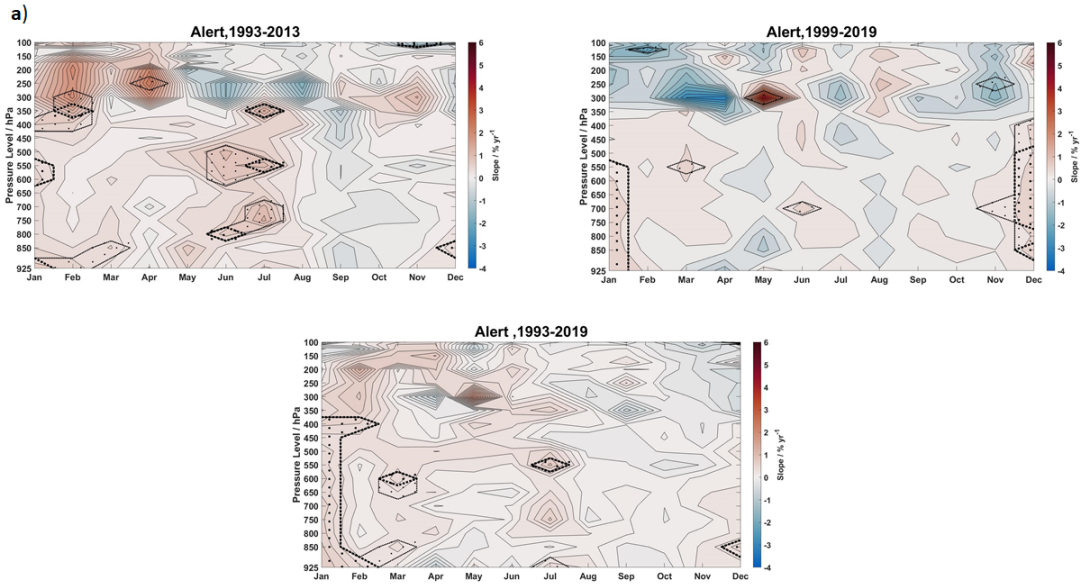


238

b)

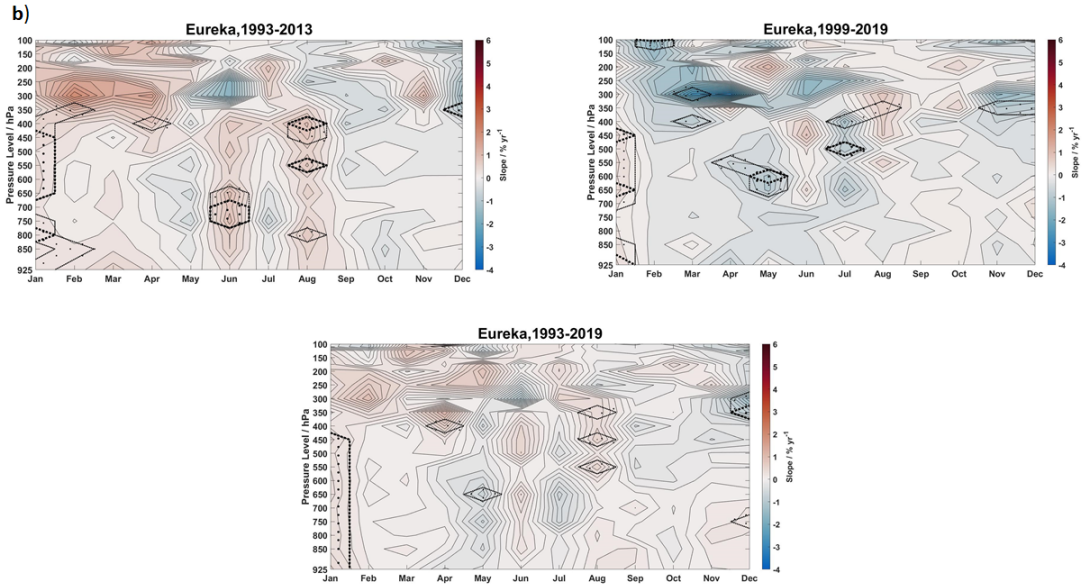


239

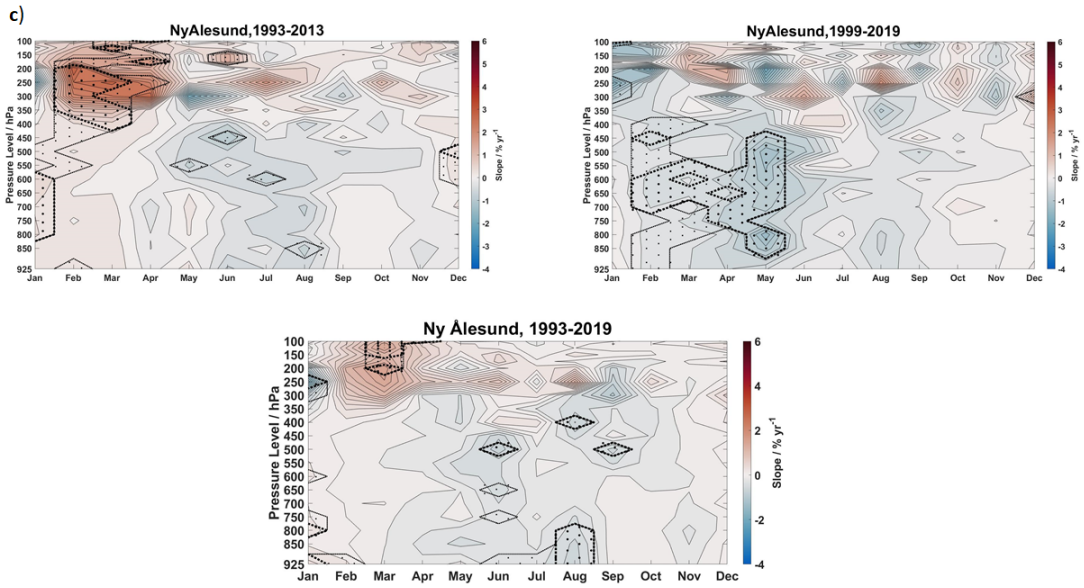
c)
NyAlesund,1993-2013
NyAlesund,1999-2019
Ny Ålesund, 1993-2019
Pressure Level / hPa
Slope / % yr-1
Jan Feb Mar Apr May Jun Jul Aug Sep Oct Nov Dec

240

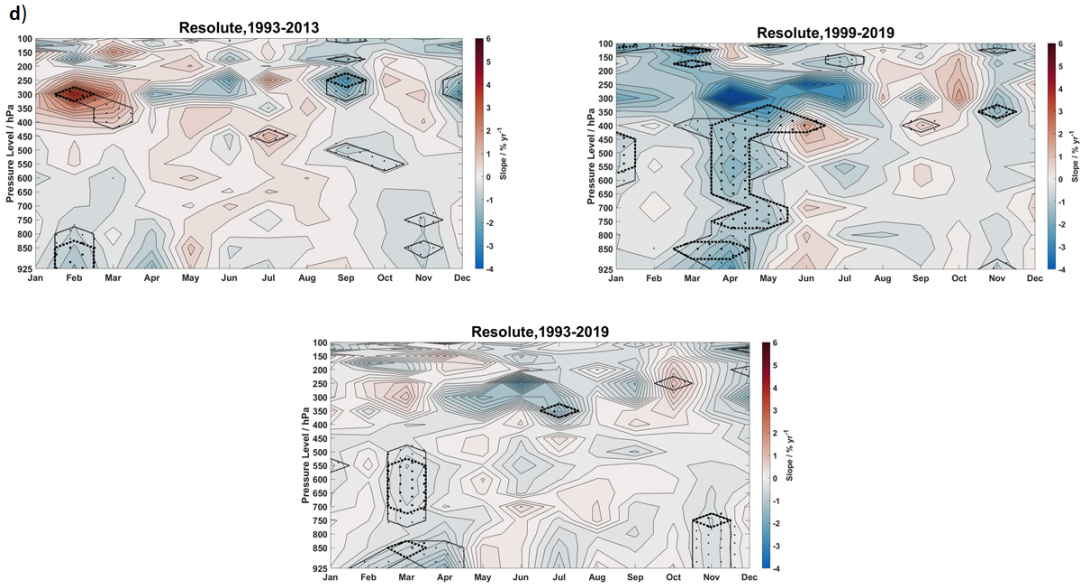
d)
Resolute,1993-2013
Resolute,1999-2019
Resolute,1993-2019
Pressure Level / hPa
Slope / % yr-1
Jan Feb Mar Apr May Jun Jul Aug Sep Oct Nov Dec

241

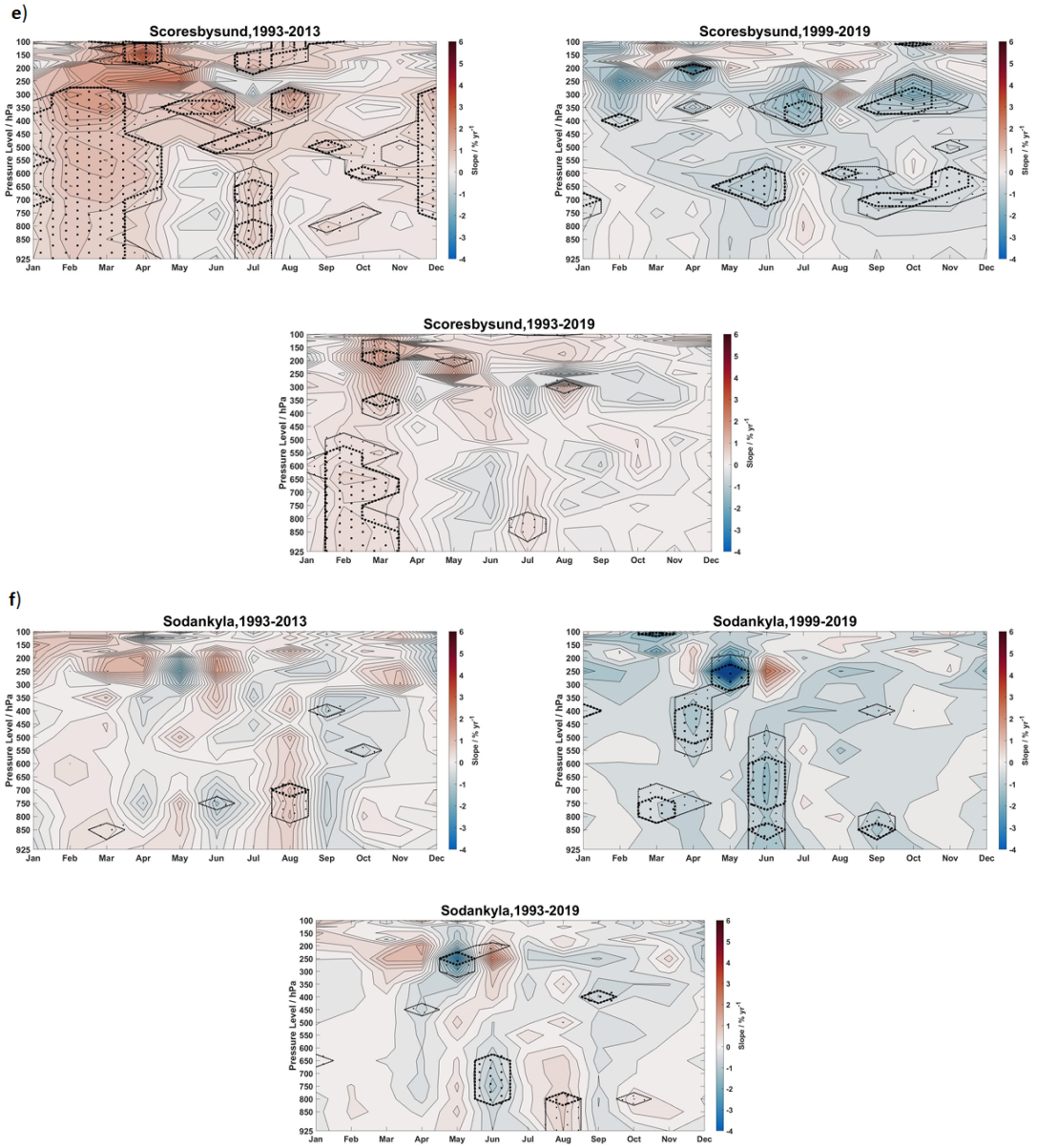


**Figure S8.** *Vertical trends in observed monthly $O_3$, relative to monthly median concentrations, in % per year, for different time periods (1993-2013, 1999-2019, and 1993-2019) from 925-100 hPa at a) Alert, b) Eureka, c) Ny Alesund, d) Resolute, e) Scoresbysund, and f) Sodankyla. Shading and symbols are the same as Fig S7a.*

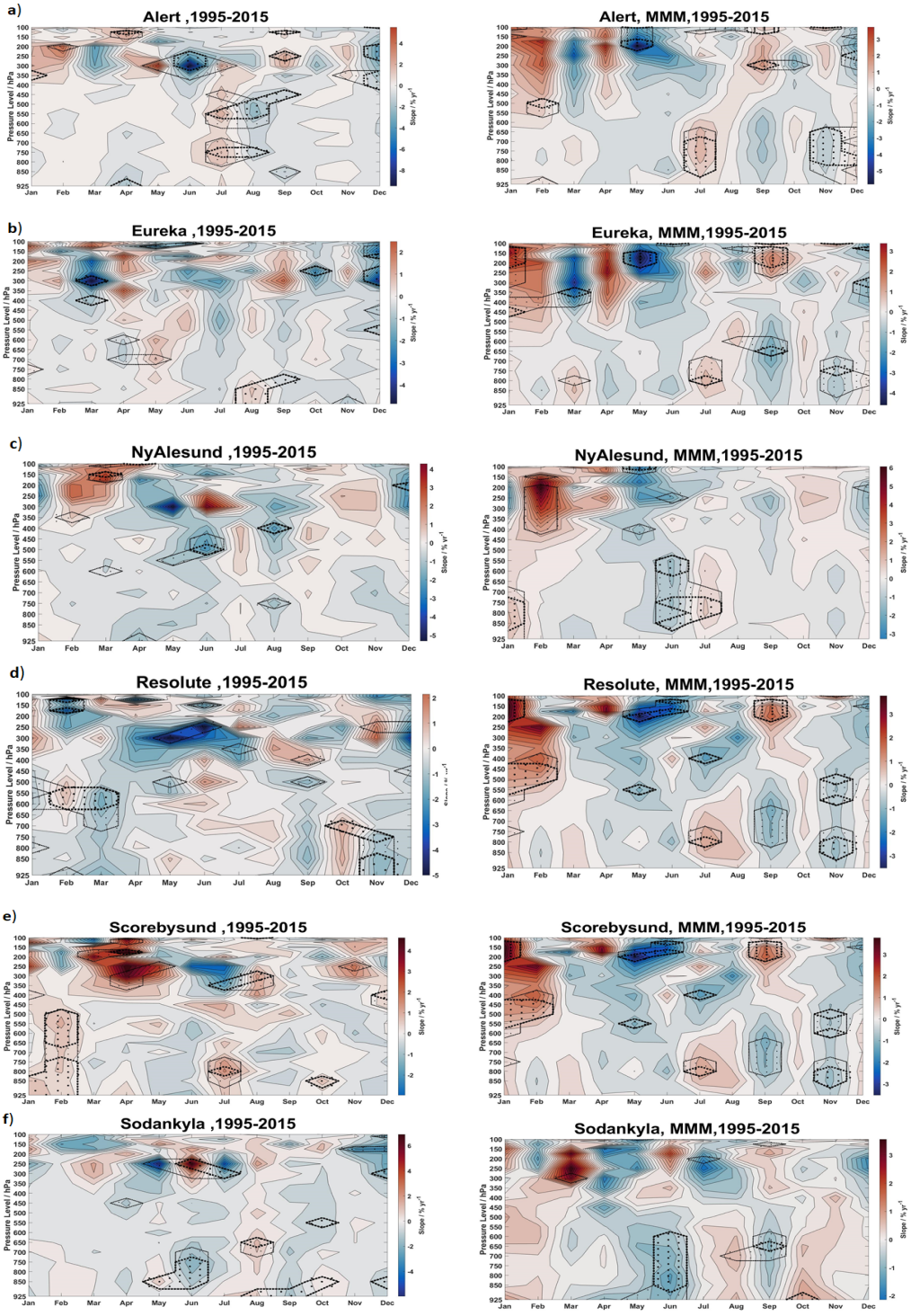


**Figure S9:** *Comparison of observed (left) and MMM (right) vertical trends in monthly $O_3$, relative to monthly medians, in % per year, from 925-100 hPa over 1995-2015 at a) Alert, b) Eureka, c) Ny Alesund, d) Resolute, e) Scoresbysund, and f) Sodankyla. Shading/symbols are the same as Fig. S7a.*

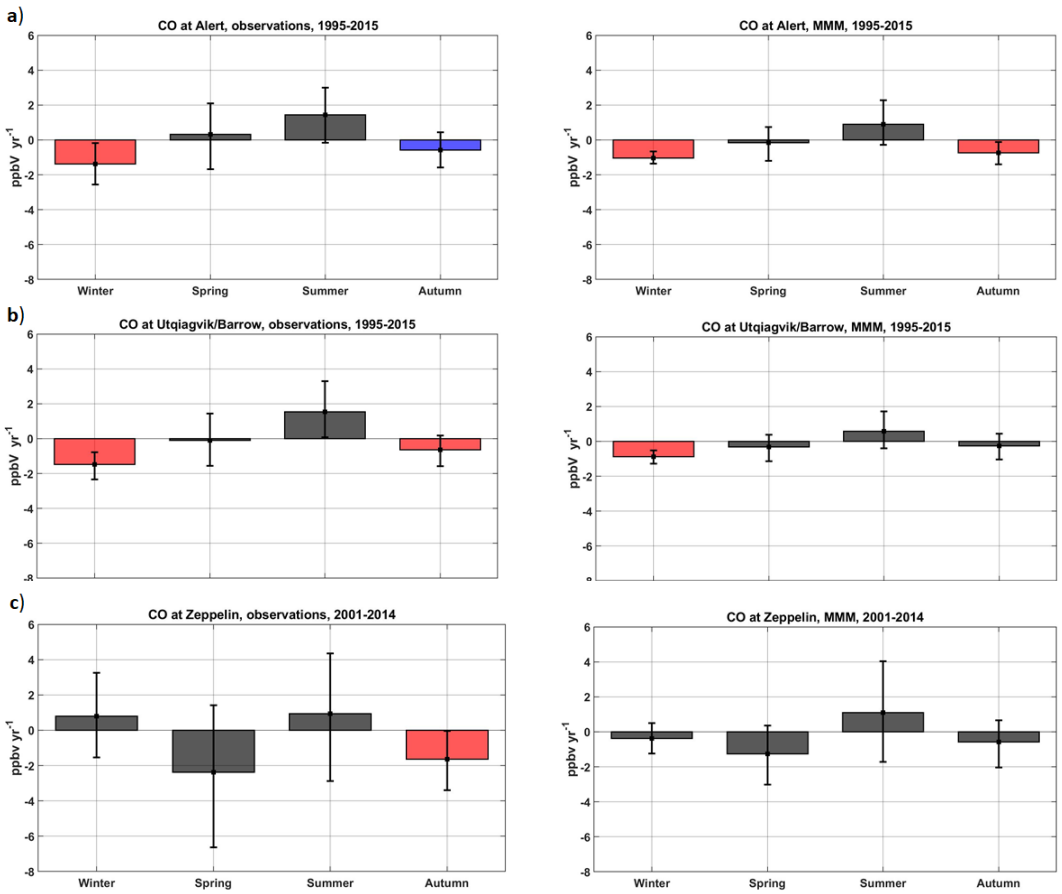


256

257

258 **Figure S10.** *Observed (left) and MMM (right) seasonal surface CO trends at a) Alert, b)*
259 *Utqiagvik, and c) Zeppelin. Boxes represent the slope of the trend in ppbv per year with red boxes*
260 *significant at 95$^{th}$ % CL, blue boxes at 90$^{th}$ % CL, and black boxes not statistically significant.*
261 *Error bars show 95$^{th}$ % CLs.*

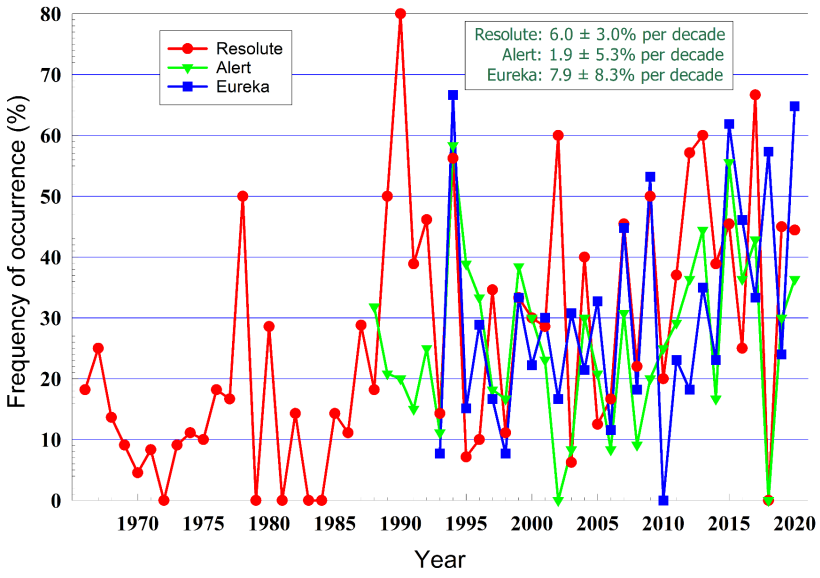


**Figure S11.** *Frequency of occurrence in % of March to May low $O_3$ concentrations, defined as <10 ppbv and indicative of $O_3$ depletion events, using ozonesonde data at the surface, and the first measurement level after balloon release, at Canadian Arctic sites from 1966–2020. Data are adjusted for the effects of occasional variation in sounding frequency. Details about the methodology are given in Tarrasick and Bottenheim (2002).*

**Table S1.** *Emissions and meteorology used in the models. See Whaley et al. (2022) for further details.*

| **Model name** | **Biogenic emissions** | **Forest fire emissions** | **Meteorology** |
|---|---|---|---|
| CMAM | None | CMIP6 | Nudged to ERA-Interim reanalysis |
| DEHM | MEGANv2 | GFAS | Nudged to ERA-Interim reanalysis |
| EMEP MSC-W | EMEP scheme (Simpson et al., 2012) | FINN (based on Wiedinmyer et al., 2011) | Driven by 3-hourly data from the Integrated Forecast System (IFS) at ECMWF |
| GISS-E2.1 | Isoprene:Guenther et al. (2012); Terpenes: ORCHIDEE; Online DMS, Sea-salt and dust | CMIP6 | Nudged to NCEP reanalysis |
| MRI-ESM2 | Biogenic VOCs emissions are taken from Horowitz et al. (2003) | CMIP6 | Nudged to the Japanese 55-year Reanalysis (JRA55) |
| UKESM1 | Isoprene and monoterpenes interactive with land surface vegetation scheme | Prescribed from CMIP6 dataset | Nudged to ERA-Interim reanalysis |

**Table S2.** *Annual surface $O_3$ trends in % per year based at Arctic sites. 'Significance level' is the probability that the observed trend is not the result of random variations. Lower and upper 95 % CLs are also shown together with the significance (confidence) level for the annual trends calculated over the periods indicated. Statistically significant trends (above 90% CL) are in bold. The far right column displays the number of years included in the trend calculation compared to the maximum number of years over the period considered.*

| Site | Annual trend (%) | Lower 95% CL | Upper 95% CL | Significance level | Period | Number yrs included/ max. yrs |
|---|---|---|---|---|---|---|
| Alert | **0.29** | 0.00 | 0.75 | 95% | 1999-2019 | 16/21 |
| | **0.24** | 0.00 | 0.60 | 95% | 1993-2019 | 22/27 |
| Utqiagvik | 0.53 | -0.32 | 1.18 | <90% | 1999-2019 | 20/21 |
| | 0.26 | -0.21 | 0.76 | <90% | 1993-2019 | 26/27 |
| Villum | **1.98** | 0.09 | 3.11 | 95% | 1999-2019 | 16/21 |
| | 0.68 | -0.28 | 2.30 | <90% | 1996-2019 | 18/24 |
| Zeppelin | -0.19 | -0.45 | 0.15 | <90% | 1999-2019 | 20/21 |
| | **0.18** | -0.03 | 0.46 | 90% | 1993-2019 | 26/27 |
| Summit | -0.28 | -0.77 | 0.12 | <90% | 2001-2019 | 19/19 |
| Esrange | 0.08 | -0.37 | 0.64 | <90% | 1999-2019 | 21/21 |
| | 0.00 | -0.24 | 0.38 | <90% | 1993-2019 | 27/27 |
| Pallas | **-0.30** | 0.85 | -0.06 | 90% | 1999-2019 | 21/21 |
| | **-0.40** | -0.84 | 0.00 | 90% | 1995-2019 | 25/25 |
| Tustervatn | **-0.52** | -1.14 | -0.08 | 99% | 1999-2019 | 21/21 |
| | -0.18 | -0.51 | 0.08 | <90% | 1994-2019 | 26/26 |

**Supplementary Information References:**


AMAP. (2015). AMAP Assessment 2015: Black carbon and ozone as Arctic climate forcers. *Arctic Monitoring and Assessment Programme (AMAP)*, 116, ISBN 978-82-7971-092-9. https://www.amap.no/documents/doc/amap-assessment-2015-black-carbon-and-ozone-as-arctic-climate-forcers/1299

AMAP (2021). AMAP Assessment 2021: Impacts of short-lived climate forcers on Arctic climate, air quality, and human health. Arctic Monitoring and Assessment Programme (AMAP), Tromsø, Norway, in press, 2023. Last access 24 January 2023. https://www.amap.no/documents/doc/amap-assessment-2021-impacts-of-short-lived-climate-forcers-on-arctic-climate-air-quality-and-human-health/3614

Collaud Coen, M., Andrews, E., Bigi, A., Martucci, G., Romanens, G., Vogt, F. P. A., and Vuilleumier, L. (2020) Effects of the prewhitening method, the time granularity, and the time segmentation on the Mann–Kendall trend detection and the associated Sen's slope, *Atmospheric Measurement Techniques, 13*, 6945-6964. https://doi/org/10.5194/amt-13-6945-2020

Collaud Coen M. and Vogt F.P.(2008), mannkendall/Matlab: Bug fix: prob_mk_n (v1.1.0). Zenodo. https://doi.org/10.5281/zenodo.4495589

296 Gautrois, M., Brauers, T., Koppmann, R., Rohrer, F., Stein, O., and Rudolph, J. (2003).
297 Seasonal variability and trends of volatile organic compounds in the lower polar
298 troposphere. *Journal of Geophysical Research: Atmospheres*, 108(D13).
299 https://doi.org/10.1029/2002JD002765

300 Gilbert, R. O. (1987) Statistical methods for environmental pollution monitoring, Van
301 Nostrand Reinhold Company, New York. ISBN 0-442-23050-8, 336pp.

302 Guenther, A. B., Jiang, X., Heald, C. L., Sakulyanontvittaya, T., Duhl, T., Emmons, L. K., &
303 Wang, X. (2012). The Model of Emissions of Gases and Aerosols from Nature version 2.1
304 (MEGAN2.1): an extended and updated framework for modeling biogenic emissions.
305 *Geoscientific Model Development*, 5(6), 1471–1492. https://doi.org/10.5194/gmd-5-1471-
306 2012

307 Helmig, D., Petrenko, V., Martinerie, P., Witrant, E., Röckmann, T., Zuiderweg, et al.
308 (2014) Reconstruction of Northern Hemisphere 1950–2010 atmospheric non-methane
309 hydrocarbons, *Atmospheric Chemistry and Physics*, 14, 1463–1483.
310 https://doi.org/10.5194/acp-14-1463-2014

311 Hirsch, R. M., Slack, J. R., and Smith, R. A. (1982) Techniques of trend analysis for
312 monthly water quality data, *Water Resources Research*, 18, 107-121.
313 https://doi.org/10.1029/WR018i001p00107

314 Horowitz, L. W., Walters, S., Mauzerall, D. L., Emmons, L. K., Rasch, P. J., Granier, C., et
315 al. (2003). A global simulation of tropospheric ozone and related tracers: Description and
316 evaluation of MOZART, version 2. *Journal of Geophysical Research: Atmospheres*,
317 108(D24). https://doi.org/10.1029/2002JD002853

318 Kulkarni, A., & von Storch, H. (1995) Monte Carlo experiments on the effect of serial
319 correlation on the Mann-Kendall test of trend, *Meteorologische Zeitschrift, 4(2),* 82-85.
320 https://doi.org/10.1127/metz/4/1992/82

321 Law, K. S., Stohl, A., Quinn, P. K., Brock, C. A., Burkhart, J. F., Paris, J.-D., et al. (2014).
322 Arctic air pollution: New insights from POLARCAT-IPY. *Bulletin of the American*
323 *Meteorological Society*, 95(12), 1873–1895. https://doi.org/10.1175/bams-d-13-00017.1

324 Mackie, A.R., P.I. Palmer, J.M. Barlow, D.P. Finch, P. Novelli and L. Jaeglé (2016)
325 Reduced Arctic air pollution due to decreasing European and North American emissions,
326 *Journal of Geophysical Research-Atmospheres*, 121, 8692-8700.
327 https://doi:10.1002/2016JD024923

328 Marelle, L., Thomas, J. L., Raut, J.-C., Law, K. S., Jalkanen, J.-P., Johansson, L., et al.
329 (2016) Air quality and radiative impacts of Arctic shipping emissions in the summertime in
330 northern Norway: from the local to the regional scale, *Atmospheric Chemistry and Physics,*
331 16, 2359–2379. https://doi.org/10.5194/acp-16-2359-2016

Pernov, J. B., Bossi, R., Lebourgeois, T., Nojgaard, J. K., Holzinger, R., Hjorth, J. L., & Skov, H. (2021). Atmospheric VOC measurements at a High Arctic site: characteristics and source apportionment. *Atmospheric Chemistry and Physics*, 21(4), 2895–2916. https://doi.org/10.5194/acp-21-2895-2021

Salmi, T., Maatta, A., Anttila, P., Ruoho-Airola, T. and Amnell, T. (2002) Detecting trends of annual values of atmospheric pollutants by the Mann-Kendall test and Sen's slope estimates - the Excel template application MAKESENS. *Finnish Meteorological Institute*, 35pp., report FMI-AQ-31, https://www.researchgate.net/publication/259356944

Sen, P. K. (1968), Estimates of the Regression Coefficient Based on Kendall's Tau, *Journal of the American Statistical Association,* 63, 1379-1389. https://doi.org/10.1080/01621459.1968.10480934

Simpson, D., Benedictow, A., Berge, H., Bergström, R., Emberson, L. D., Fagerli, H., et al. (2012). The EMEP MSC-W chemical transport model - technical description. *Atmospheric Chemistry and Physics*, 12(16), 7825–7865. https://doi.org/10.5194/acp-12-7825-2012

Tarasick, D.W., and J.W Bottenheim (2002) Surface ozone depletion episodes in the Arctic and Antarctic from historical ozonesonde records, *Atmospheric Chemistry and Physics, 2*, 197-205, https://doi.org/10.5194/acp-2-197-2002

Theil, H. (1950) A rank-invariant method of linear and polynomial regression analysis, *Proceedings Nederlandse Akademie van Wetenschappen,* 53, 386-392. https://ir.cwi.nl/pub/18446

Walker, T. W., Jones, D. B. A., Parrington, M., Henze, D. K., Murray, L. T., Bottenheim, J. W., et al. (2012). Impacts of midlatitude precursor emissions and local photochemistry on ozone abundances in the Arctic. *Journal of Geophysical Research-Atmospheres*, 117. https://doi.org/10.1029/2011jd016370

Wang, W., Chen, Y., Becker, S., & Liu, B. (2015) Variance correction prewhitening method for trend detection in autocorrelated data, *Journal of Hydrologic Engineering*, 20, 04015033. https://doi:10.1061/(ASCE)HE.1943-5584.0001234

Whaley, C. H., Mahmood, R., von Salzen, K., Winter, B., Eckhardt, S., Arnold, et al. (2022), Model evaluation of short-lived climate forcers for the Arctic Monitoring and Assessment Programme: a multi-species, multi-model study, *Atmospheric Chemistry and Physics, 22*, 5775–5828. https://doi.org/10.5194/acp-22-5775-2022

Whaley, C. H., Law, K. S., Hjorth, J. L., Skov, H., Arnold, S. R., Langner, J., Pernov, et al. (2023), Arctic tropospheric ozone: assessment of current knowledge and model performance. *Atmospheric Chemistry and Physics*, 23, 637-661. https://doi.org/10.5194/acp-23-637-2023

Wiedinmyer, C., Akagi, S. K., Yokelson, R. J., Emmons, L. K., Al-Saadi, J. A., Orlando, J. J., & Soja, A. J. (2011). The Fire INventory from NCAR (FINN): a high resolution global model to estimate the emissions from open burning. *Geoscientific Model Development*, 4(3), 625–641. https://doi.org/10.5194/gmd-4-625-2011

Yue, S., and Wang, C. Y. (2002) Applicability of prewhitening to eliminate the influence of serial correlation on the Mann-Kendall test, *Water Resources Research, 38*, 4-1-4-7, https://doi.org/10.1029/2001WR000861